Available online at www.sciencedirect.com
ScienceDirect
Journal of Organometallic Chemistry 692 (2007) 2456–2472
Journal of Organometallic Chemistry
www.elsevier.com/locate/jorganchem

Synthesis and characterization of transition metal stabilized carbocations of the types $[Cp^*(CO)_2Fe\{\mu\text{-}(C_nH_{2n-1}\}M(CO)_xCp]PF_6$ ($x = 2$, M = Fe or Ru; $x = 3$, M = W, $Cp^* = \eta^5\text{-}C_5(CH_3)_5$; $Cp = \eta^5\text{-}C_5H_5$; $n = 3$–6) and $[Cp(CO)_2Ru\{\mu\text{-}(C_nH_{2n-1})\}W(CO)_3Cp]PF_6$ ($n = 3$–5) and the crystal structures of the complexes $[Cp^*(CO)_2Fe(CH_2)_3Ru(CO)_2Cp]$, $[Cp^*(CO)_2Fe(CH_2)_5Ru(CO)_2Cp]$, $[Cp^*(CO)_2Fe\text{-}(CH_2)_5W(CO)_3Cp]$, and $[Cp(CO)_2Ru(CH_2)_5W(CO)_3Cp]$

Evans O. Changamu [a], Holger B. Friedrich [a,*], Melanie Rademeyer [b]

[a] School of Chemistry, University of KwaZulu-Natal, Durban 4041, South Africa
[b] School of Chemistry, University of KwaZulu-Natal, Private Bag X01, Scottsville, Pietermaritzburg 3209, South Africa

Received 13 December 2006; received in revised form 11 February 2007; accepted 15 February 2007
Available online 21 February 2007

Abstract

The mixed-ligand complexes $[Cp^*(CO)_2Fe(CH_2)_nM(CO)_xCp]$ ($x = 2$, M = Fe or Ru; $x = 3$, M = W, $Cp^* = \eta^5\text{-}C_5(CH_3)_5$; $Cp = \eta^5\text{-}C_5H_5$; $n = 3$–6), type **I**, react with one equivalent of the hydride abstractor Ph_3CPF_6 to give the transition metal-stabilized carbocation complexes $[Cp^*(CO)_2Fe\{\mu\text{-}(C_nH_{2n-1})\}M(CO)_xCp]PF_6$. Similarly the new heterobimetallic complexes $[Cp(CO)_2Ru\{\mu\text{-}(C_nH_{2n-1})\}\text{-}W(CO)_3Cp]$, type **II**, react with Ph_3CPF_6 to give the carbocation complexes $[Cp(CO)_2Ru\{\mu\text{-}(C_nH_{2n-1})\}W(CO)_3Cp]PF_6$. Spectroscopic data show that hydride abstraction selectively takes place from the methylene group β to the metal atom attached to the Cp^* ligand in type **I** complexes. In type **II** complexes, the reaction is totally metalloselective with hydride abstraction occurring at the CH_2 β to the ruthenium metal centre. All products have been characterized by IR, ^1H,^{13}C NMR spectroscopy and elemental analysis. ^1H and ^{13}C NMR data clearly show that in the carbocation complexes one metal is σ-bonded to the alkanediyl carbocation while the other is bonded to the cationic end in a η^2-fashion forming a chiral metallacylopropane type structure. The molecular structures of the cationic metallacyclic complexes $[Cp^*(CO)_2Fe\{\mu\text{-}(C_3H_5)\}Fe(CO)_2Cp]PF_6$ [E.O. Changamu, H.B. Friedrich, M. Rademeyer, Acta Crystallogr., Sect. E 62 (2006) m442.] and $[Cp^*(CO)_2Fe(\mu\text{-}C_3H_5)Ru\text{-}(CO)_2Cp]PF_6$ [H.B. Friedrich, E.O. Changamu, M. Rademeyer, Acta Crystallogr., Sect. E 62 (2006) m405.] have been confirmed by single crystal X-ray crystallography and reported elsewhere. The structures of the precursor complexes $[Cp^*(CO)_2Fe(CH_2)_3Ru\text{-}(CO)_2Cp]$ (**1**), $[Cp^*(CO)_2Fe(CH_2)_5Ru\text{-}(CO)_2Cp]$ (**2**), $[Cp^*(CO)_2Fe(CH_2)_5W(CO)_3Cp]$ (**3**), and $[Cp(CO)_2Ru\ (CH_2)_5W(CO)_3Cp]$ (**4**), have been confirmed by single crystal X-ray crystallography. The structure of $[Cp^*(CO)_2\text{-}Fe(CH_2)_3Ru(CO)_2Cp]$ is compared with that of its corresponding cationic complex, $[Cp^*(CO)_2Fe\{\mu\text{-}(C_3H_5)\}Ru(CO)_2Cp]PF_6$.

Keywords: Alkanediyl carbocation, Mixed-ligand; Heterobimetallic; Metallacyclopropane; Hydride abstraction

1. Introduction

Whereas mononuclear complexes of the types $[Cp(CO)_2M(\eta^2\text{-}CH_2{=}CHR)]X$ (M = Fe or Ru) and $[Cp^*(CO)_2Fe(\eta^2\text{-}CH_2{=}CHR)]X$($Cp = \eta^5\text{-}C_5H_5$, $Cp^* = \eta^5\text{-}C_5(CH_3)_5$, R = alkyl or aryl group, X = BF_4 or PF_6) have

* Corresponding author. Tel.: +27 31 2603107; fax: +27 31 2603091.
E-mail address: friedric@ukzn.ac.za (H.B. Friedrich).

0022-328X/$ - see front matter © 2007 Elsevier B.V. All rights reserved.
doi:10.1016/j.jorganchem.2007.02.016

been fairly well studied [3–11], there are very few reports of their bimetallic analogues in which both Cp and Cp* ligands are present in the same molecule. Furthermore, there are very few reports of heterodinuclear organometallic carbocations in the literature that have no metal–metal bonds [1,2,12].

Transition metal stabilized carbocations were believed to be cationic metal olefin complexes [6,7,10,12–15], which are strongly activated towards nucleophilic attack [16]. This phenomenon plays a key role in many important catalytic processes [17]. Transition metal olefin complexes are also considered to be models for catalytic intermediates in important industrial processes like metathesis, oligomerization and polymerization of alkenes and alkynes, hydration and oxidation of olefins and hydroformylation. Furthermore, there are reports that heterobimetallic catalysts are considered superior to their monometallic analogues in activity and selectivity [18]. A deeper understanding of the nature of the bonding in the reactive intermediates of these processes should give more insight into the mechanisms of the catalytic reactions.

The bonding between unsaturated hydrocarbons and transition metals is usually treated as donor–acceptor in nature and is mostly described in terms of the Dewar–Chatt–Duncanson (DCD) model [19,20]. The validity of the DCD model has been supported by both experiment and theory [21–23], but more recent studies suggest that the model is not suited to quantify the distortion of the ligand in the complex or to predict the details of the bonding properties of different ligands [24]. For example, it does not distinguish between a π-bonded complex and a metallacycle as an alternative description of the three-membered cyclic structure. The latter is suggested to be prevalent in high oxidation state organometallic complexes [25]. Very recent experimental and theoretical studies by Scherer et al. on valence shell charge concentrations in olefin complexes of nickel also suggest that the nature of bonding between olefins and transition metals may be more complex than portrayed by the DCD model [26].

Our recent NMR studies on the complexes $[\{Cp(CO)_2Fe\}_2(\mu\text{-}C_nH_{2n-1})]PF_6$ ($n = 4$–10) and $[\{Cp(CO)_2Fe\}_2(\mu\text{-}C_nH_{2n-2})](PF_6)_2$ ($n = 5$–10) showed that the metals form metallacyclopropane type structures with the cationic end of the alkanediyl carbocation and that the positive charge is distributed mainly within the metallacycle [27]. These studies demonstrated that NMR spectroscopy may be used to distinguish between the traditional side-on bonding between unsaturated hydrocarbons and transition metals and the three-membered metallacycle. The metallacyclopropane complexes are chiral, with the β-CH carbon being the chiral centre. The chirality is observed in the ^1H NMR spectra in which the protons of the methylene groups attached to the chiral centre (γ-CH_2) are observed to be diastereotopic [1,2,6,27]. In some complexes this effect is also observed in the protons of the methylene group that is β to the chiral centre [6,27]. This effect is unlikely to be observed in side-on bonded ligands in which there is free rotation around the metal–ligand axis and the C_β–C_γ bond (see Fig. 1). Furthermore, X-ray diffraction studies have shown that the molecular geometries of the complexes $[Cp^*(CO)_2Fe\{\mu\text{-}(C_3H_5)\}Fe(CO)_2Cp]PF_6$ and $[Cp^*(CO)_2Fe\{\mu\text{-}(C_3H_5)\}Ru(CO)_2Cp]PF_6$ ($Cp^* = \eta^5\text{-}C_5Me_5$) are significantly distorted at the β-$CH^{\delta+}$ position to allow for greater interaction between the metal centre and the β-$CH^{\delta+}$ carbon resulting in the formation of chiral metallacyclopropane type structures [1,2].

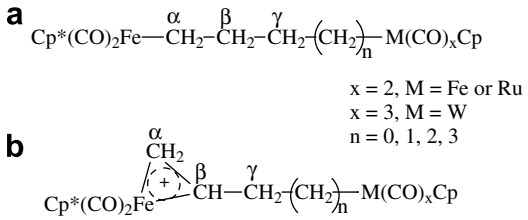

Fig. 1. Structural formula of (a) alkanediyl complex (b) transition metal-stabilized metallacyclic carbocation complex showing the labeling of carbon positions of the hydrocarbon ligand.

We now report on a series of the mixed-ligand transition metal alkanediyl complexes $[Cp^*(CO)_2Fe(CH_2)_nM(CO)_x\text{-}Cp]$ (where $n = 3$–6; $x = 2$, M = Fe, or Ru, $x = 3$, M = W) and $[Cp(CO)_2Ru(CH_2)_nW(CO)_3Cp]$ ($n = 3$–5) and their reactions with Ph_3CPF_6 to give the transition metal-stabilized carbocations $[Cp^*(CO)_2Fe\{\mu\text{-}(C_nH_{2n-1})\}M(CO)_x\text{-}Cp]PF_6$ (where $n = 3$–6; $x = 2$, M = Fe, or Ru, $x = 3$, M = W) and $[Cp(CO)_2Ru\{\mu\text{-}(C_nH_{2n-1})\}W(CO)_3Cp]PF_6$ ($n = 3$–5). The precursor complexes $[Cp^*(CO)_2Fe(CH_2)_nM\text{-}(CO)_xCp]$ (where $x = 2$, $n = 3$, M = Fe, $n = 3$–5, M = Ru) have been reported previously [28], but the rest are new.

2. Results and discussion

2.1. Preparation of the complexes $[Cp^*(CO)_2Fe\{\mu\text{-}(C_nH_{2n-1})\}M(CO)_xCp]PF_6$ (n = 3–6; x = 2, M = Fe or Ru; x = 3, M = W)

Reactions of the neutral complexes $[Cp^*(CO)_2Fe(CH_2)_n\text{-}M(CO)_xCp]$ (M = Fe, W or Ru, $n = 3$–6) with Ph_3CPF_6 in CH_2Cl_2 gave deep red solutions from which the carbocation complexes $[Cp^*(CO)_2Fe\{\mu\text{-}(C_nH_{2n-1})\}M(CO)_xCp]PF_6$ were obtained by precipitation with diethyl ether in good yields (32–89%). The solutions of tungsten containing complexes appeared bluish-green indicating partial decomposition. The complexes where $n = 3$ were precipitated as orange microcrystalline solids, while the rest of the complexes separated as red oils upon addition of diethyl ether to the CH_2Cl_2 solutions. The red oils swelled up into pale yellow, almost clear, spongy solids, which were found to be analytically pure after drying under reduced pressure. These have low melting points reminiscent of ionic liquids, as they consist of large cations, $[Cp^*(CO)_2Fe\{\mu\text{-}(C_nH_{2n-1})\}ML_y]^+$, associated with a relatively small counter anion PF_6^-.

The complexes where $n = 3$ are fairly stable in air at 5 °C. For example, a sample of $[Cp^*(CO)_2Fe\{\mu\text{-}(C_3H_5)\}Fe(CO)_2Cp]PF_6$ was kept in the fridge at 5 °C for seven months with minimal decomposition. However, they decompose in solution to brown solids, especially if the solvents are not nitrogen-saturated. The complexes where $n > 3$ darken and become sticky when exposed to air, but are stable for several months under nitrogen at −15 °C. They are more soluble in halogenated solvents than the complexes where $n = 3$ and solubility increases with increase carbocation chain length. All the compounds have been characterized by ^1H and ^{13}C NMR spectroscopy, IR spectroscopy and elemental analysis and data are given in Tables 1–3. The structures of $[Cp^*(CO)_2Fe\{\mu\text{-}(C_3H_5)\}Fe(CO)_2Cp]PF_6$ and $[Cp^*(CO)_2Fe\{\mu\text{-}(C_3H_5)\}Ru(CO)_2Cp]PF_6$ have been confirmed by single crystal X-ray crystallography and have been reported elsewhere [1,2]. The structures show significant distortion in the molecular geometry resulting from enhanced interaction between the metal attached to the Cp^* ligand and the β-CH^+ group. The ^{13}C NMR data also support this observation and are discussed in Section 2.1.3.

2.1.1. IR spectroscopy

The IR spectral data are summarized in Table 1. The complexes show two bands in the C–O stretching region within the range 2053–2013 cm^{-1}, which are assignable to the cationic $Cp^*(CO)_2Fe$ carbonyls. These values are in agreement with reported data for related mononuclear complexes [6]. Two other expected bands lie within the range 2003–1946 cm^{-1}, with positions characteristic of the metal to which the CO groups are attached [28]. In this range some of the compounds show only one strong and broad band, probably because of band overlap.

2.1.2. ^1H NMR spectroscopy

The ^1H NMR spectroscopic data are summarized in Table 2. The data show that hydride abstraction took place selectively from the CH_2 group β to the Fe attached to the Cp^* ligand. For example, the characteristic triplet in the spectra of the neutral precursors, $[Cp^*(CO)_2Fe(CH_2)_nM(CO)_xCp]$ ($x = 2$, M = Fe or Ru; $x = 3$, M = W; $n = 3$–6), at around 0.9 ppm due to the equivalent protons of the CH_2 α to the $Cp^*(CO)_2Fe$ group is absent from the spectra of the carbocation complexes. The position of the peak assignable to the Cp protons in the carbocation complexes is also not significantly different from the one observed in the neutral complexes. Apart from the iron and ruthenium-containing complexes where $n = 3$, all the complexes show two characteristic sharp doublets at about 2.82 ppm ($J \sim 8.1$ Hz) and 3.05 ppm ($J \sim 14.4$ Hz) assignable to the diastereotopic CH_2 protons α to the $Cp^*(CO)_2Fe$ group. These protons do not show geminal coupling. In all the complexes the γ-CH_2 protons show separate multiplets in the spectra. This is expected because they are in the neighbourhood of a chiral centre (the β-CH carbon). Similarly, the δ-CH_2 (see Fig. 1) protons show separate multiplets in the spectra as would be expected for protons in the neighbourhood of a prochiral centre (the γ-CH_2). These assignments were confirmed by 2D NMR experiments including HSQC, COSY and NOESY. The spectra are similar to those of $[Cp^*(CO)_2Fe\{\mu\text{-}(C_3H_5)\}Fe(CO)_2Cp]PF_6$ recorded at −50 °C, where the molecule is expected to be static (see Fig. 3, Section 2.4). The molecular structures of the complexes $[Cp^*(CO)_2Fe\{\mu\text{-}(C_3H_5)\}Fe(CO)_2Cp]PF_6$ [2] and $[Cp^*(CO)_2Fe\{\mu\text{-}(C_3H_5)\}Ru(CO)_2Cp]PF_6$ [1] show that the metal attached to the Cp^* ligand is coordinated to the alkanediyl carbocation in a η^2-fashion forming metallacyclopropane type structures, with the bond Fe–C_β being 2.302(6) Å and 2.291(3) Å, respectively. The data, therefore, suggest that the same type of bonding prevails in the longer chain complexes.

In the spectrum of $[Cp^*(CO)_2Fe\{\mu\text{-}(C_3H_5)\}W(CO)_3Cp]PF_6$ the diastereotopic $FeCH_2$ protons show sharp and well-resolved doublets with $J \approx 7.9$ and 14.7 Hz, respectively. The sharpness of these signals and the cou-

Table 1
Data for $[Cp^*(CO)_2Fe(C_nH_{2n-1})ML_y]PF_6$

n	ML_y	Yield (%)	Mp. (°C)	IR ν(CO)/(cm^{-1})[a]	Elemental analysis	
					C: Found (calculated)	H: Found (calculated)
3	$CpFe(CO)_2$	82	130–133	2042m, 2016m, 1966m	43.3 (43.2)	4.1 (4.1)
4	$CpFe(CO)_2$	80	48–51	2053m, 2011m, 1949m	44.1 (44.2)	4.2 (4.3)
5	$CpFe(CO)_2$	60	44–47	2051m, 2024m, 1945s	45.4 (45.1)	4.3 (4.5)
6	$CpFe(CO)_2$	64	94–96	2055m, 2016m, 2003s, 1942m	45.7 (46.0)	4.6 (4.8)
3	$CpRu(CO)_2$	89	119–120	2042m, 2025m, 2000s, 1970s	39.7 (40.3)	3.8 (3.6)
4	$CpRu(CO)_2$	82	38–40	2052s, 2015s, 1952s	40.9 (41.3)	4.0 (4.0)
5	$CpRu(CO)_2$	32	40–42	2054s, 2014s, 1948s	42.3 (42.1)	4.3 (4.2)
6	$CpRu(CO)_2$	68	68–70	2055s, 2016s, 2003sh, 1941s	43.3 (43.1)	4.6 (4.6)
3	$CpW(CO)_3$	51	88–90	2045s, 2021s, 2004sh, 1920sbr	35.8 (36.1)	3.3 (3.3)
4	$CpW(CO)_3$	78	65–67	2053s, 2018s, 1972m, 1915sbr	36.6 (36.9)	3.5 (3.5)
5	$CpW(CO)_3$	57	62–63	2055s, 2013s, 1911s	38.4 (37.8)	3.4 (3.7)
5[b]	$CpW(CO)_3$	80	150–152	2055, 2014, 1912	58.1 (58.5)	5.0 (4.9)
6	$CpW(CO)_3$	63	46–48	2055s, 2012s, 1910s	38.6 (38.9)	3.9 (3.9)

[a] Measured in CH_2Cl_2.
[b] Counter ion is BPh_4^-; s = strong, sbr = strong and broad, sh = shoulder, m = medium.

Table 2
^{1}H NMR data for $[Cp^*(CO)_2Fe(C_nH_{2n-1})ML_y]PF_6$

n	ML_y	CpM	Cp^*Fe	*cis*-$FeCH_2$($^3J_{HH}$)[e]	*trans*-$FeCH_2$	$FeCH_2CH$	$FeCH_2CHCH_2$	MCH_2	MCH_2CH_2	$MCH_2CH_2CH_2$
3	$CpFe(CO)_2$[a]	5.16 (5H, s)	1.97 (15H, s)	2.58 (1H, m)	3.05 (1H, d, 12.8)	5.48 (1H, m)		2.52 (1H, m), 1.65 (1H, m)		
4	$CpFe(CO)_2$[c]	4.78 (5H, s)	1.87 (15H, s)	2.75 (1H, d, 7.9)	3.03 (1H, d, 14.4)	4.02 (1H, m)	1.22(1H, m), 2.26 (1H, m)	1.75 (1H, m), 1.08 (1H, m)		
5	$CpFe(CO)_2$[c]	4.76 (5H, s)	1.88 (15H, s)	2.85 (1H, d, 8.1)	3.11 (1H, d, 14.5)	3.92 (1H, m)	2.35 (1H, m), 1.15 (1H, m)	1.35 (2H, m)	1.45 (1H, m), 1.69 (1H, m)	
5[d]	$CpFe(CO)_2$[a]	4.94 (5H, s)	2.10 (15H, s)	3.15 (1H, d, 8.2)	3.44 (1H, d, 14.4)	4.30 (1H, m)	2.47 (1H, m), 1.32 (1H, m)	1.45 (2H, m)	1.52 (1H, m), 1.86 (1H, m)	
6	$CpFe(CO)_2$[c]	4.72 (5H, s)	1.88 (15H, s)	2.83 (1H, d, 8.1)	3.08 (1H, d, 14.7)	3.89 (1H, m)	2.30 (1H, m), 1.23 (1H, m)	1.38 (2H, m)	1.46 (2H, m)	1.69 (1H, m), 1.34 (1H, m)
3	$CpRu(CO)_2$[a]	5.61 (5H, s)	1.96 (15H, s)	2.54 (1H, m)	2.97 (1H, m)	5.66 (1H, m)		2.21 (2H, m), 2.90 (2H, m)		
4	$CpRu(CO)_2$[b]	5.37 (5H, s)	1.86 (15H, s)	2.80 (1H, d, 8.1)	3.14 (1H, d, 14.4)	4.02 (1H, m)	2.41 (1H, m), 1.50 (1H, m)	1.44 (1H, m), 1.95 (1H, m)		
5	$CpRu(CO)_2$[c]	5.25 (5H, s)	1.88 (15H, s)	2.84 (1H, d, 7.9)	3.11 (1H, d, 14.3)	3.92 (1H, m)	2.33 (1H, m), 1.13 (1H, m)	1.52 (2H, m)	1.88 (1H, m), 1.52 (1H, m)	
6	$CpRu(CO)_2$[c]	5.22 (5H, s)	1.88 (15H, s)	2.83 (1H, d, 8.1)	3.08 (1H, d, 14.3)	3.89 (1H, m)	2.29 (1H, m), 1.32 (1H, m)	1.58 (2H, m)	1.58 (2H, m)	1.58 (1H, m), 1.32 (1H, m)
3	$CpW(CO)_3$[a]	5.82 (5H, s)	1.98 (15H, s)	2.62 (1H, d, 7.8)	3.19 (1H, d, 14.6)	5.23 (1H, m)		2.94 (1H, m), 1.96 (1H, m)		
4	$CpW(CO)_3$[c]	5.44 (5H, s)	1.88 (15H, s)	2.80 (1H, d, 8.0)	3.03 (1H, d, 14.4)	4.06 (1H, m)	2.38 (1H, m), 1.30 (1H, m)	1.75 (1H, m), 1.21 (1H, m)		
5	$CpW(CO)_3$[c]	5.42 (5H, s)	1.89 (15H, s)	2.86 (1H, d, 6.5)	3.14 (1H, d, 14.4)	3.98 (1H, m)	2.33 (1H, m)	1.63 (1H, m), 1.15 (1H, m)	1.63 (2H, m)	
5[d]	$CpW(CO)_3$[a]	5.65 (5H, s)	2.04 (15H, s)	3.16 (1H, d, 8.2)	3.45 (1H, d, 13.4)	4.29 (1H, m)	2.46 (1H, m), 1.42 (1H, m)	1.62–1.79 (4H, m)		
6	$CpW(CO)_3$[c]	5.38 (5H, s)	1.88 (15H, s)	2.84 (1H, d, 8.2)	3.11 (1H, d, 14.5)	3.92 (1H, m)	2.31 (1H, m), 1.23 (1H, m)	1.44 (2H, m)	1.55 (2H, m)	1.61 (1H, m), 1.36 (1H, m)

[a] Recorded in acetone-d_6.
[b] Recorded in CD_3CN.
[c] Recorded in $CDCl_3$.
[d] Counter ion is BPh_4^-.
[e] J values are given in Hz.

Table 3
^{13}C NMR data for $[Cp^*(CO)_2Fe(C_nH_{2n-1})ML_y]PF_6$

n	ML_y	MCO	Cp^*FeCO	CpM	$C_5(CH_3)_5$	$FeCH_2$	$FeCH_2CH$	$FeCH_2CH\ CH_2$	MCH_2	MCH_2CH_2	$MCH_2CH_2CH_2$	$C_5(CH_3)_5$
3	$CpFe(CO)_2$[a]	N.O.	N.O.	87.0	100.2	45.2	118.8		10.2			9.0
4	$CpFe(CO)_2$[b]	217.1, 217.0	212.4, 212.2	85.5	101.7	55.8	89.7	44.6	5.3			9.2
5	$CpFe(CO)_2$[b]	217.6, 217.5	212.4, 212.2	85.5	101.9	57.5	87.5	42.1	1.8	41.5		9.3
5[d]	$CpFe(CO)_2$[b]	218.9	216.5	85.6	101.4	57.6	87.6	41.4	1.5	41.4		8.2
6	$CpFe(CO)_2$[b]	217.7	212.3	85.4	102.1	57.3	87.7	36.5	2.1	37.5	37.6	9.3
3	$CpRu(CO)_2$[a]	201.5	N.O.	90.2	100.3	44.3	119.6		6.6			9.4
4	$CpRu(CO)_2$[c]	203.4	213.7, 213.1	89.9	102.2	57.0	90.8	46.4	−0.9			9.4
5	$CpRu(CO)_2$[b]	202.3, 202.1	212.4, 212.3	88.6	101.9	57.5	87.6	42.2	−5.2	42.9		9.3
6	$CpRu(CO)_2$[b]	202.5	212.4, 212.2	88.6	102.0	57.4	87.8	36.5	−4.8	37.5	39.0	9.4
3	$CpW(CO)_3$[a]	218.4	219.6, 229.7	91.9	94.8	18.9	44.9		−4.7			8.2
4	$CpW(CO)_3$[b]	N.O.	N.O.	91.8	101.5	56.3	90.9		−9.3	43.6		9.3
5	$CpW(CO)_3$[b]	228.6, 218.2, 218.1	212.5, 212.1	91.7	101.8	57.8	87.7	43.1	−12.5	40.2		9.3
5[d]	$CpW(CO)_3$[a]	229.2, 219.5	212.2,	92.1	101.4	57.7	87.2	42.4	−12.7	40.2		8.2
6	$CpW(CO)_3$[b]	218.1	212.2, 212.1	91.6	101.9	57.5	87.9	36.2	−11.7	36.1	38.7	9.2

[a] Recorded in acetone-d_6.
[b] Recorded in $CDCl_3$.
[c] Recorded in CD_3CN.
[d] Counter ion is BPh_4^-, N.O. = not observed.

pling constants suggest that the chirality of the β-carbon is maintained even in solution and that this compound does not undergo a detectable dynamic process in solution. Similar observations have been made in the heterobimetallic complex $[Cp(CO)_2Ru\{\mu\text{-}(C_3H_5)\}W(CO)_3Cp]PF_6$ (Section 2.2.2).

2.1.3. ^{13}C NMR spectroscopy

The ^{13}C NMR data are summarized in Table 3 and they support the conclusion that hydride abstraction occurred selectively from the CH_2 that is β to the $Cp^*(CO)_2Fe$ in spite of the steric demands of the bulky Ph_3C^+ and Cp^* groups. For example, the signal observed at around 14 ppm assignable to the carbon atom of the CH_2 α to $Cp^*(CO)_2Fe$ in the spectra of the starting materials, $[Cp^*(CO)_2Fe(CH_2)_nM(CO)_xCp]$ ($x = 2$, M = Fe or Ru; $x = 3$, M = W; $n = 3$–6), is significantly shifted to about 57 ppm in the spectra of the carbocation complexes. Furthermore, the signals assignable to the $Cp(CO)_2M$ carbonyl and Cp carbon atoms are similar to those reported for related neutral complexes [28], whilst the signals assignable to the $Cp^*(CO)_2Fe$ group carbonyl and Cp^* carbon atoms are shielded and deshielded, respectively. These data agree closely with those reported for related cationic mononuclear complexes [6]. This further confirms that hydride abstraction occurred from the CH_2 group β to the bulky $Cp^*(CO)_2Fe$ group. This is not unexpected given the electron releasing ability of the methyl groups of the Cp^* ligand, which increases the π-donor ability of the Fe atom to which it is attached. The increased π-donor ability of the metal labilises the β-CH_2 hydride more than the metal atom attached to the Cp ligand on the other end of the alkyl bridge, making it to be more readily abstracted by the Ph_3C^+ electrophile. In the product, the increased π-donor ability of the metal and the increased acceptor ability of the hydrocarbon ligand favour strong interaction between the two. This may lead to the distortion of the hydrocarbon ligand and formation of a strong bond. This distortion has been observed [1,2] and is discussed alongside the structure of the neutral complex $[Cp^*(CO)_2Fe\text{-}(CH_2)_3Ru(CO)_2Cp]$ in Section 2.3.

The position of the signal assignable to the β-CH^+ carbon shifts to higher field as the chain length of the alkanediyl carbocation increases. The shift is most significant when the alkanediyl carbocation chain length increases from $n = 3$ to $n = 4$. Thus, in the complex where $n = 3$ the β-CH^+ carbon atoms resonate at about 118, while in the complex where $n = 4$ the β-CH^+ carbon atoms resonate at about 90 ppm i.e. shielding of about 28 ppm by just increasing the alkanediyl carbocation chain length by one methylene group. In the complexes where $n > 4$, the β-CH^+ carbons resonate at about 88 ppm corresponding to shielding of about 2 ppm relative to the complexes where $n = 4$. As the alkanediyl carbocation chain length increases there is reduced steric interaction between the Cp and Cp^* ligands, which allows the metal and the β-CH^+ carbon to approach each other more closely resulting in a stronger

interaction, which is probably responsible for the increase in the shielding experienced by the β-CH^+ carbon.

Another remarkable observation is the very small degree of deshielding experienced by the carbon atom of the γ-CH_2 group (see Fig. 1b). For example, in the neutral complex $[Cp^*(CO)_2Fe(CH_2)_3Fe(CO)_2Cp]$, the carbon of the CH_2 α to $Fe(CO)_2Cp$ (γ to $Cp^*(CO)_2Fe$) resonates at 9.4 ppm (in $CDCl_3$) [28], while in the cationic metallacyclic complex $[Cp^*(CO)_2Fe\{\mu\text{-}(C_3H_5)\}Fe(CO)_2Cp]PF_6$ it resonates at 9.8 ppm (in $CDCl_3$). Thus, it is deshielded by only 0.4 ppm relative to the starting material. In contrast, the β-CH_2 carbon is deshielded by about ~74 ppm, while the carbon of CH_2 α to $Cp^*(CO)_2Fe$ is deshielded by 26 ppm relative to the neutral complex. In the complex $[Cp^*(CO)_2Fe(CH_2)_4Fe(CO)_2Cp]$, the γ-$CH_2$ carbon resonates at 43.6 ppm (see Section 4.3), while in the cationic metallacyclic complex $[Cp^*(CO)_2Fe\{\mu\text{-}(C_4H_7)\}Fe(CO)_2Cp]PF_6$ it resonates at 44.6 ppm. Thus, it is deshielded by only 1 ppm relative to the neutral complex. In contrast, the β-CH_2 carbon is deshielded by about 44 ppm, while the α-CH_2 carbon is deshielded by about 42 ppm relative to the neutral complex. This trend is observed in all the other complexes and can only be attributed to increased back-donation from the metal atom to the β-CH^+, which effectively diminishes the negative inductive effect on the γ-CH_2 carbon. This also indicates that the positive charge is distributed mainly among the groups forming the metallacyclopropane ring. This further supports the representation of the bonding between the metal centre and the alkanediyl carbocation as shown in Fig. 1(b), rather than the traditional side-on DCD model [19,20].

2.2. Preparation of the complexes $[Cp(CO)_2Ru\{\mu\text{-}(C_nH_{2n-1})\}W(CO)_3Cp]PF_6 (n = 3–5)$

The new neutral Ru–W heterobimetallic complexes $[Cp(CO)_2Ru(CH_2)_nW(CO)_3Cp]$ were prepared by reacting the ruthenium complexes $[Cp(CO)_2Ru(CH_2)_nI]$ ($n = 3$–5) with the salt $Na[Cp(CO)_3W]$ in THF. The characterization data of these new compounds are reported in Section 4.9. They were reacted with Ph_3CPF_6 in CH_2Cl_2 to give orange red solutions from which the corresponding cationic metallacyclic complexes $[Cp(CO)_2Ru\{\mu\text{-}(C_nH_{2n-1})\}W(CO)_3Cp]PF_6$ were precipitated as pale yellow, air-stable microcrystalline solids by the addition of diethyl ether. These complexes are insoluble in most hydrocarbon solvents such as hexane and halogenated solvents such as chloroform. They are, however, fairly soluble in acetone, nitromethane and THF.

2.2.1. IR spectroscopy

The IR spectral data are summarized in Table 4. These complexes show four C–O stretching bands: two in the range 2084–2041 cm^{-1}, assignable to cationic Ru–CO carbonyls, and two others in the range 2011–1911 cm^{-1}, assignable to the neutral W–CO carbonyls. These values are in close agreement with reported data for related compounds [12,28,29].

2.2.2. ^1H NMR spectroscopy

The ^1H NMR spectroscopic data are summarized in Table 5. The data show that hydride abstraction occurred at the ruthenium side of the alkyl chain. In general the spectra show the same pattern as those of the mixed-ligand complexes. The main difference is in the positions of the chemical shifts assignable to the $RuCH_2$ protons. In these complexes the protons that show *cis* coupling with the β-CH proton (the proton of the CH_2 α to Ru) are more deshielded than those that show *trans* coupling. In contrast, in the mixed-ligand complexes (Section 2.1.3) these positions are reversed. The spectrum of the complex where $n = 3$ is significantly different from those of its mixed-ligand analogues $[Cp^*(CO)_2Fe\{\mu\text{-}(C_3H_5)\}Fe(CO)_2Cp]PF_6$ and $[Cp^*(CO)_2Fe\{\mu\text{-}(C_3H_5)\}Ru(CO)_2Cp]PF_6$, in that the diastereotopic $RuCH_2$ protons show sharp and well-resolved doublets with J values of 4.8 and 14.3 Hz, respectively. In this respect, it is similar to the mixed-ligand tungsten-containing analogue $[Cp^*(CO)_2Fe\{\mu\text{-}(C_3H_5)\}W(CO)_3Cp]PF_6$. The sharpness of these signals suggests that the chirality of the β-carbon is maintained even in solution and that this complex is more static than some of its mixed-ligand analogues.

2.2.3. ^{13}C NMR spectroscopy

These data are summarized in Table 6. They support the conclusion that hydride abstraction took place selectively at the Ru side of the alkyl chain. For example, the signal assignable to the carbon of the CH_2 α to the $Cp(CO)_2W$ metal appears only slightly deshielded in the spectra of the cationic metallacyclic complexes relative to the corresponding neutral complexes, $[Cp(CO)_2Ru(CH_2)_nW(CO)_3Cp]$. On the other hand, the α and β carbon atoms on the Ru side are significantly deshielded in the cationic metallacyclic complexes relative to the neutral starting materials, which strongly suggests that the positive charge is located on the Ru side of the molecule. This may be attributed to the ruthenium centre being less sterically crowded than the tungsten centre. Hence, the ruthenium is likely to interact more strongly with the β-CH_2 than the tungsten and thus labilise a hydride, which is then abstracted by the trityl salt, resulting in the formation of a distorted tetragonal pyramidal structure.

2.3. The molecular structure of the neutral complex $[Cp^*(CO)_2Fe(CH_2)_3Ru(CO)_2Cp]$ (**1**)

The molecular structure of **1** in Fig. 2 shows two crystallographically independent molecules found in the asymmetric unit. In each molecule, the Fe and Ru atoms are coordinated in a pseudo-octahedral fashion, with the Fe atom coordinated by two carbonyls, the η^5-pentamethylcyclopentadienyl ligand and the alkyl chain. The Ru atom is coordinated by two carbonyls, a η^5-cyclopentadienyl ligand and the bridging alkyl chain. The alkyl chain adopts the energetically favoured all-*trans* conformation. With respect to the Fe attached to the Cp^* ligand the β-carbon

Table 4
Data for $[Cp(CO)_2Ru(C_nH_{2n-1})W(CO)_3]PF_6$

n	Yield (%)	Decomposing temperature (°C)	IR ν(CO)/(cm^{-1}) in CH_2Cl_2	Elemental analysis	
				C: Found (calculated)	H: Found (calculated)
3	59	>118	2069, 2024, 1924	29.7 (29.2)	2.1 (2.0)
4	52	>107	2084, 2054, 2015, 1913	30.4 (30.2)	2.5 (2.3)
5	54	>95	2083, 2041, 2011, 1911	31.7 (31.2)	2.8 (2.5)

of the alkyl chain lies in a conformation between the two CO ligands, while with respect to the ruthenium centre it lies in a conformation between a CO ligand and the Cp ligand. This conformational preference with respect to the Cp* ligand has been observed in reported mononuclear complexes containing the Cp* ligand [30,31]. The conformation with respect to the Cp ligand is common with alkyl and alkanediyl Cp containing complexes [29,32,33]. The direct consequence of this conformations in the same molecule is that the Cp* ligand is approximately perpendicular to the alkyl chain, while the Cp on the Ru atom is parallel to the same alkyl chain plane. In this way the rings are far apart, thus reducing steric interaction.

The Fe–C_α bond lengths of 2.06(3) Å and 2.11(2) Å of the independent molecules in the asymmetric unit of compound **1** are similar to 2.057 Å and 2.069 Å reported for $Cp^*(CO)_2Fe(CH_2)_3Br$ [30] and $Cp^*(CO)_2Fe(n\text{-}C_5H_{11})$ [31], respectively. The Ru–C_α bond lengths of 2.13(2) Å and 2.17(2) Å in compound **1** are within the range of 2.142–2.179 Å reported for $[Cp(CO)_2Fe(CH_2)_3Ru(CO)_2Cp]$ [29] and $[Cp(CO)_2Ru(CH_2)_5Ru(CO)_2Cp]$ [34]. Important bond lengths and angles are summarized in Table 7.

The torsion angles Fe1–C11–C12–C13 = 177.2(17)°, Ru1–C13–C12–C11 = −161.6(18)°, C33–C34–C35–Ru2 = 162.8(17)° are close to 180°, confirming that the metals are σ-bonded to the alkyl chain [33].

In Table 8 selected bond angles and bond lengths of the neutral complex **1** (molecule A) are compared with those of the corresponding cationic metallacyclic complex, $[Cp^*(CO)_2Fe\{\mu\text{-}(C_3H_5)\}Ru(CO)_2Cp]PF_6$ (**1a**). It can be seen that there is significant distortion in the molecular geometry around the Fe centre in compound **1a**. For example, in going from compound **1** to **1a**, the angle C12–C11–Fe (i.e. C_β–C_α–Fe) decreased from 117.5(18)° to 76.51(14)°. On the other hand, the angle C11–C12–Fe (i.e. C_α–C_β–Fe) increased from the non-bonded 36.85° to the bonded 67.23°. The Fe–C12 (i.e. Fe–C_β) bond distance decreased from the non-bonded 3.05 Å in **1** to the bonded 2.291(3) Å in **1a**. This is significantly shorter than 2.59 Å and 2.72 Å reported for the carbocation complex $[\{Cp(CO)_2Fe\}_2\{\mu\text{-}C_3H_5)\}]PF_6$ [32]. These observations suggest a significant shortening of the Fe–C12 (i.e. Fe–C_β) distance and hence strong interaction between the metal centre and the β-CH^+ carbon. The bond length Fe–C11 (i.e. Fe–C_α) increased from 2.06(3) Å in **1** to 2.173(2) Å in **1a**. The C11–C12–C13 bond angle of the alkyl group increased from the more tetrahedral 114°in **1** to the distorted 125° in the cationic metallacyclic complex **1a**. Thus, there is significant distortion in the molecular geometry after hydride abstraction, resulting in stronger interaction between the metal and the β-CH^+ carbon.

The foregoing observations confirm the suggestions made by Cais et al. that organometallic carbocations are stabilized by the delocalization of the positive charge and the ability of the molecule to undergo geometrical changes, which result in enhanced bonding interaction between the metal atom and the formally positive ligand moiety [35].

2.4. Variable temperature NMR studies on $[Cp^*(CO)_2Fe\{\mu\text{-}(C_3H_5)\}Fe(CO)_2Cp]PF_6$

The ^1H NMR spectrum of the complex $[Cp^*(CO)_2Fe\{\mu\text{-}(C_3H_5)\}Fe(CO)_2Cp]PF_6$ showed five broad peaks assignable to the five protons of the C_3H_5 moiety (Table 2). The broadening of the peaks in the spectrum was possibly due to the molecule undergoing a dynamic process in solution. Fig. 3a shows a stacked plot of some of the spectra recorded at various temperatures. It can be seen that all the signals assignable to the α-CH_2 protons of the C_3H_5 moiety (H_{trans}, H_{cis}, H_a and H_b) broadened and then collapsed into the baseline at temperatures above 40 °C.

Below 15 °C the peaks assignable to the protons of the CH_2 group α to the $Cp^*(CO)_2Fe$ group (H_{trans} and H_{cis}) resolve into sharp doublets. The separate peaks assigned to the protons of the CH_2 group α-to the $Cp(CO)_2Fe$ group (H_a and H_b) resolved into a multiplet at 2.55 ppm and a doublet of doublets at 1.65 ppm, respectively. There was no further change observed in the spectrum at temperatures below 0 °C. This showed that the dynamic process responsible for peak broadening was ''frozen out'' rather easily by lowering the temperature of the solution slightly below room temperature. At all the temperatures the Cp^* and Cp ligand peaks remained sharp singlets. We had hoped that the diasteriotopic α-CH_2 protons would coalesce into doublets at a temperature above room temperature but the compound decomposed before this was observed.

At temperatures above room temperature, the signal at 5.5 ppm (assignable to the β-CH^+ proton) sharpened and resolved into an almost binomial quintet (see Fig. 4). This suggested that the metallacyclopropane ring observed in solution at room temperature and in the solid state may have opened. At temperatures below room temperature, this multiplet became broad and less resolved.

To further probe the changes in the spectra at temperatures above room temperature, the solvent was changed

Table 5
^{1}H NMR data for $[Cp(CO)_2Ru(C_nH_{2n-1})W(CO)_3Cp]PF_6$ in $CDCl_3$

n	CpRu	CpW	*cis*-$RuCH_2$ ($^3J_{HH}$)[a]	*trans*-$RuCH_2$	$RuCH_2CH$	$RuCH_2CH\ CH_2$	WCH_2	WCH_2CH_2
3	6.14 (5H, s)	5.91 (5H, s)	3.52 (1H, d, 4.8)	3.93 (1H, d, 14.3)	6.4 (1H, m)		2.9 (1H, m), 2.3 (1H, m)	
4	6.23 (5H, s)	5.78 (5H, s)	3.99 (1H, d, 8.3)	3.93 (1H, d, 14.0)	5.5 (1H, m)	2.7 (1H, m), 1.5 (1H, m)	1.9 (2H, m)	
5	6.23 (5H, s)	5.78 (5H, s)	4.42 (1H, d, 8.3)	3.99 (1H, d, 14.0)	5.4 (1H, m)	2.5 (1H, m), 1.6 (1H, m)	1.8 (2H, m)	1.9 (1H, m), 1.7 (1H, m)

[a] Coupling constants are given in Hz.

from acetone-d_6 to dimethylformamide-d_7 (DMF). The spectra obtained at all temperatures were the same as those observed in acetone, apart from insignificant changes in the chemical shift positions. However, it was observed that when the temperature was raised above 70 °C, even the signal assignable to the β-CH^+ proton disappeared, suggesting that the compound may have decomposed or the carbocation may have been displaced by the coordinating DMF solvent. Solvent coordination and subsequent olefin displacement has been reported involving acetonitrile as the solvent in hydride abstraction reactions [7]. In the present case the spectra show some evidence to support the presence of $[Cp(CO)_2FeCH_2CH{=}CH_2]$ in solution. For example, a new multiplet at about 6.00 ppm assignable to the =CH proton in $[Cp(CO)_2FeCH_2CH{=}CH_2]$, two doublets between 4.46 and 4.78 ppm assignable to the $=CH_2$ protons and a doublet at 2.10 ppm assignable to $FeCH_2$ protons appeared. Resonances assignable to the dimers $[Cp^*(CO)_2Fe]_2$ and $[Cp(CO)_2Fe]_2$ were also observed at 1.78 ppm and 4.96 ppm, respectively, but not any derivatives of the C_3H_5 moiety. Any cyclopropane or propene formed from the decomposition or displacement may have left the solution and hence not been detected by NMR, because of the high operating temperatures.

The position of the multiplet assignable to the β-CH^+ proton shifts to higher field as the temperature is lowered (Fig. 4). This observed shielding may be due to increasing back-donation of electron density from the metal centre into the formally positively charged β-CH^+, leading to the strengthening of the metallacyclopropane structure. At lower temperatures (below 0 °C) there is increased interaction between the metal centre and the β-CH^+ carbon resulting in increased back-donation and hence shielding of the proton. At high temperatures (>50 °C) increased molecular vibration leads to opening of the metallacyclopropane ring.

2.5. Reactions of the mixed-ligand complexes $[Cp^*(CO)_2Fe\{\mu\text{-}(C_5H_9)\}M(CO)_2Cp]PF_6$ (M = Fe, Ru) with NaI and CD_3OD

The reactions of the compound $[Cp^*(CO)_2Fe\{\mu\text{-}(C_5H_9)\}Ru(CO)_2Cp]PF_6$ with both NaI and deuterated methanol, as well as the reaction between $[Cp^*(CO)_2Fe\{\mu\text{-}(C_5H_9)\}Fe(CO)_2Cp]PF_6$ and NaI, were studied as illustrations of the reactions between the mixed-ligand carbocation complexes with nucleophiles. The reactions were followed by proton NMR spectroscopy. Both the methoxide and iodide anions attack the Fe attached to the Cp^* ligand, giving $[Cp^*(CO)_2FeOCD_3]$ and $[Cp^*(CO)_2FeI]$, respectively. In addition, the new ruthenium η^1-alkenyl complex $[Cp(CO)_2Ru(CH_2)_3CH{=}CH_2]$ was obtained from $[Cp^*(CO)_2Fe\{\mu\text{-}(C_5H_9)\}Ru(CO)_2Cp]PF_6$, while the previously reported iron η^1-alkenyl complex $[Cp(CO)_2Fe(CH_2)_3CH{=}CH_2]$ [36] was obtained from $[Cp^*(CO)_2Fe\{\mu\text{-}(C_5H_9)\}Fe(CO)_2Cp]PF_6$. No addition products were observed in solution. The reactions did not go to completion after 40 min and were found to be slower that those

Table 6
^{13}C NMR data for $[Cp(CO)_2Ru(C_nH_{2n-1})W(CO)_3Cp]PF_6$ in $CDCl_3$

n	RuCO	WCO	CpRu	CpW	$RuCH_2$	$RuCH_2CH$	$RuCH_2CHCH_2$	WCH_2	WCH_2CH_2
3	N.O.	230.2, 220.1	93.9	91.9	40.6	115.8		−2.2	
4	197.1, 195.4	229.6, 219.9	93.4	92.2	50.1	89.1	45.1	−6.6	
5	197.0, 195.4	230.6, 219.9	93.3	92.3	51.8	86.1	44.0	−11.8	41.1

N.O. = not observed.

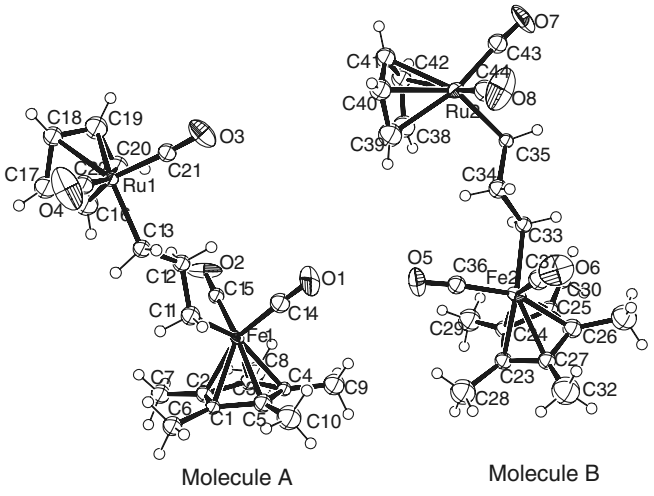

Fig. 2. The Molecular structures of the crystallographically independent molecules (A and B) in the asymmetric unit of **1** showing atom-numbering scheme.

Table 7
Selected bond lengths and angles for compound **1**

Bond length (Å)		Bond angle (°)	
C14–Fe1	1.78(3)	C15–Fe1–C14	98.8(12)
C15–Fe1	1.74(2)	C15–Fe1–C11	91.1(11)
Fe1–C11	2.06(3)	C14–Fe1–C11	85.8(12)
C13–C12	1.57(3)	C12–C11–Fe1	117.5(18)
C13–Ru1	2.13(2)	C34–C33–Fe2	116.4(17)
C22–Ru1	1.85(3)	C21–Ru1–C22	88.9(12)
C21–Ru1	1.84(3)	C21–Ru1–C13	87.1(11)
C37–Fe2	1.74(3)	C22–Ru1–C13	85.6(11)
C33–C34	1.52(4)	C21–Ru1–C19	101.6(12)
C33–Fe2	2.11(2)	C37–Fe2–C36	96.5(13)
Ru2–C44	1.88(3)	C37–Fe2–C33	87.9(12)
Ru2–C43	1.91(3)	C36–Fe2–C33	90.2(11)
Ru2–C35	2.17(2)	C44–Ru2–C43	91.5(13)
C11–C12	1.49(4)	C44–Ru2–C35	87.7(11)
C36–Fe2	1.78(3)	C43–Ru2–C35	87.4(11)
C34–C33	1.52(4)	C34–C35–Ru2	111.4(15)
C34–C35	1.54(3)	C11–C12–C13	114.0(2)

of the corresponding symmetrical complexes $[\{Cp(CO)_2Fe\}_2\{\mu\text{-}(C_nH_{2n-1})\}]PF_6$ [27]. This is attributable to stabilization by the electron releasing Cp^* ligand that enhances the π-donor ability of the Fe to the β-CH carbon.

2.6. Reactions of $[Cp^*(CO)_2Fe\{\mu\text{-}(C_5H_9)\}M(CO)_xCp]PF_6$ with $NaBPh_4$ ($x = 2$, $M = Fe$; $x = 3$, $M = W$)

The complexes $[Cp^*(CO)_2Fe\{\mu\text{-}(C_nH_{2n-1})\}M(CO)_xCp]PF_6$ (where $n = 4$–6) are low melting solids and did not give X-ray quality crystals. The reaction with $NaBPh_4$ was carried out in a bid to raise the melting points and the stability of these complexes. It was found that the complexes $[Cp^*(CO)_2Fe\{\mu\text{-}(C_5H_9)\}W(CO)_3Cp]BPh_4$ and $[Cp^*(CO)_2Fe\{\mu\text{-}(C_5H_9)\}Fe(CO)_2Cp]BPh_4$ readily form when the precursors are dissolved together in acetone and stirred briefly. They precipitate as yellow plates upon addition of diethyl ether to the CH_2Cl_2 solutions. They melt at 150–152 °C, which is significantly higher when compared with the 62–63 °C of the PF_6^- salts.

2.7. Molecular structure of the neutral complexes $[Cp^*(CO)_2Fe(CH_2)_5Ru(CO)_2Cp]$ (**2**), $[Cp^*(CO)_2Fe(CH_2)_5W(CO)_3Cp]$ (**3**) and $[Cp(CO)_2Ru(CH_2)_5W(CO)_3Cp]$ (**4**)

The above complexes are precursors to some of the carbocation complexes discussed in Sections 2.1 and 2.2. Determination of their structures by crystallography is an important step towards understanding the source of the stability exhibited by the carbocation complexes, as well as their structures. Obtaining X-ray quality crystals of the carbocation complexes remains a challenge, as they behave like ionic liquids, but a change of counter ion has shown some promising results.

The molecular structure of $[Cp^*(CO)_2Fe(CH_2)_5Ru(CO)_2Cp]$ (**2**), shown in Fig. 5 is broadly similar to that of compound **1**, the major difference being the length of the alkyl bridge between the metal centres. Compound **2** has a C_5 alkyl bridge, while compound **1** has a C_3 alkyl bridge between the metal centres. The bond length Fe–$C_{(alkyl)} = 2.063(5)$ Å is similar to 2.06(3) Å and 2.11(2) Å observed in the two independent molecules of **1**, respectively. The bond length Ru–$C_{(alkyl)} = 2.161(5)$ Å in compound **2** is similar to 2.13(2) Å and 2.17(2) Å observed in compound **1**. Selected bond angles and bond lengths are given in Table 9.

The torsion angles C11–C12–C13–C14 = 177.6(4)°, C15–C14–C13–C12 = 173.1(4)°, C13–C12–C11–Fe = 165.6(3)°, C13–C14–C15–Ru = −176.8(3)° confirm that the alkyl chain is fully saturated and σ-bonded to both metals [33].

The molecular structure of $[Cp^*(CO)_2Fe(CH_2)_5W(CO)_3Cp]$ (**3**) is shown in Fig. 6. The compound differs from compound **2** in that it contains tungsten instead of ruthenium as the second metal centre. The geometry at the tungsten atom is distorted tetragonal pyramidal in which the base is made up of the three carbonyl ligands

Table 8
Comparison between the bond distances of complex **1** and the carbocation complex **1a**

	1	**1a**[a]		**1**	**1a**[a]
Bond angle (°)			*Bond length (Å)*		
C11–C12–Fe	36.85	67.23(14)	Fe–C11	2.06(3)	2.17(2)
C12–C11–Fe	117.50 (18)	76.51(14)	Fe–C12	3.05	2.29(3)
C11–Fe–C12	25.68	36.26(8)	Fe–C14	1.78(3)	1.78(3)
C14–Fe–C15	98.80(12)	92.51(11)	Fe–C15	1.74(2)	1.79(3)
C11–C12–C13	114(2)	125.2(2)	O2–C14	1.13(4)	1.13(3)
C12–C13–Ru	115.9(16)	107.23(15)	O1–C15	1.16(3)	1.14(3)
C21–Ru–C22	88.9(12)	92.96(12)	C11–C12	1.49(4)	1.39(3)

[a] Data obtained from the CIF file of Ref. [2].

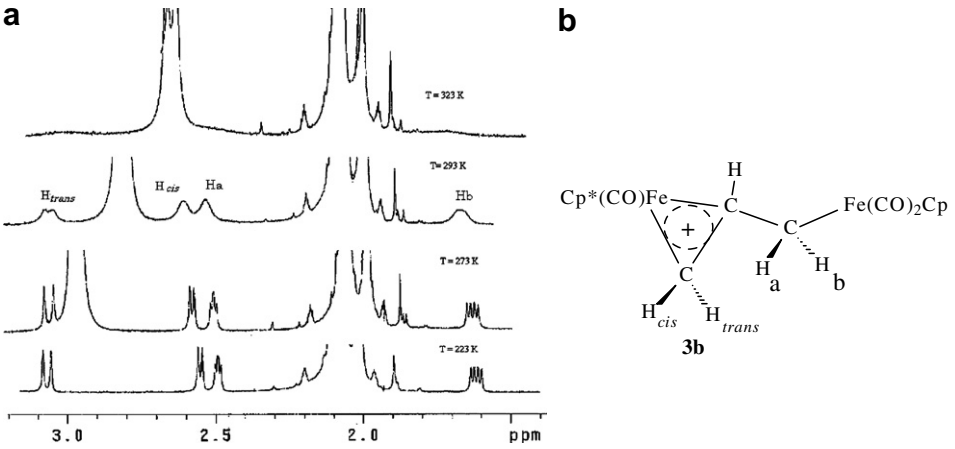

Fig. 3. (a) The stacked plot of selected ^{1}H NMR spectra of the α-CH_2 protons of C_3H_5 portion of $[Cp^*(CO)_2Fe\{\mu\text{-}(C_3H_5)\}Fe(CO)_2Cp]PF_6$ recorded between −50 and 50 °C. Labeling of protons is shown in the structure on the right side (b).

and C15 of the alkyl chain and the apex is the metal capped with the cyclopentadienyl ligand. The bond length Fe–$C_{(alkyl)}$ = 2.067(5) Å is similar to the values observed in **1** and **2**. The bond length W–$C_{(alkyl)}$ = 2.321(6) Å is within the range expected for W–$C_{(alkyl)}$ bond distances reported for related compounds [30]. W–$C_{(CO)}$ vary from 1.960(6)–1.981(6) Å and are within the ranges reported for related compounds [30]. Selected bond angles and bond lengths are given in Table 9.

Compounds **2** and **3** are precursors to the cationic metallacyclic complexes $[Cp^*(CO)_2Fe\{\mu\text{-}(C_5H_9)\}Ru(CO)_2Cp]PF_6$ and $[Cp^*(CO)_2Fe\{\mu\text{-}(C_5H_9)\}W(CO)_3Cp]PF_6$. Even though the structures of the cationic metallacyclic complexes have not been confirmed by X-ray crystallography, ^{13}C NMR data of the cationic metallacyclic complexes

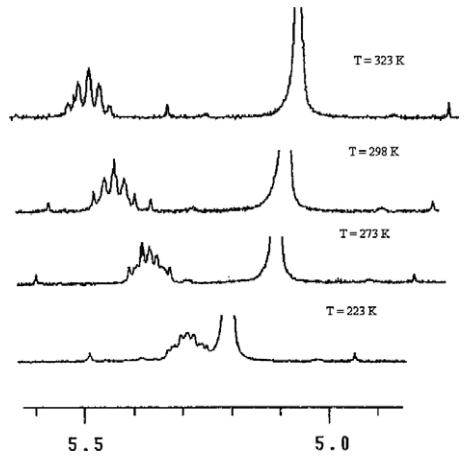

Fig. 4. The stacked plot of selected ^{1}H NMR spectra of the β-CH proton of $[Cp^*(CO)_2Fe\{\mu\text{-}(C_3H_5)\}Fe(CO)_2Cp]PF_6$ recorded between −50 and 50 °C.

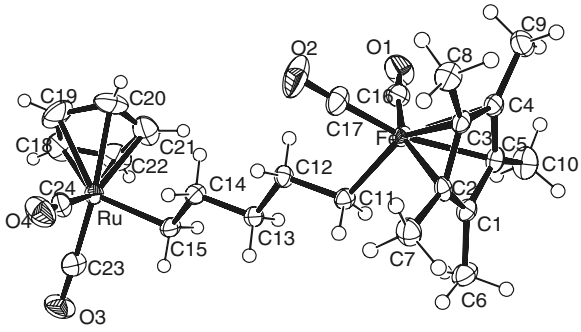

Fig. 5. The molecular structure of $[Cp^*(CO)_2Fe(CH_2)_5Ru(CO)_2Cp]$ (**2**) showing the atom numbering scheme.

Table 9
Selected bond lengths (Å) and bond angles (°) of compounds **2**, **3** and **4**

2		**3**		**4**		**2**		**3**		**4**	
Bond length (Å)						*Bond angle (°)*					
Fe–C11	2.063(5)	Fe1–C11	2.067(5)	C20–Ru1	1.85(2)	C17–Fe–C16	97.3(3)	C17–Fe1–C16	93.9(3)	C21–Ru1–C20	92.3(7)
Fe–C16	1.754(6)	Fe1–C16	1.760(6)	C21–Ru1	1.847(19)	C17–Fe–C11	88.3(2)	C17–Fe1–C11	89.4(2)	C21–Ru1–C10	85.9(7)
Fe–C17	1.745(5)	Fe1–C17	1.747(6)	C10–Ru1	2.138(16)	C16–Fe–C11	90.0(2)	C16–Fe1–C11	90.2(2)	C20–Ru1–C10	87.9(8)
C16–O2	1.160(6)	C16–O1	1.141(7)	C11–W1	1.968(16)	C12–C11–Fe	117.2(3)	C12–C11–Fe1	118.4(4)	C9–C10–Ru1	116.5(12)
C17–O1	1.149(7)	C17–O2	1.157(7)	C12–W1	1.992(18)	C11–C12–C13	114.6(4)	C11–C12–C13	115.0(4)	C6–C7–C8	113.2(14)
Ru–C15	2.161(5)	W1–C15	2.321(6)	C13–W1	1.969(17)	C12–C13–C14	112.2(4)	C12–C13–C14	110.1(5)	C7–C8–C9	113.4(14)
Ru–C23	1.851(6)	W1–C23	1.960(6)	C6–W1	2.320(16)	C13–C14–C15	114.0(4)	C13–C14–C15	113.3(5)	C10–C9–C8	113.4(13)
Ru–C24	1.859(6)	W1–C24	1.981(6)	O5–C21	1.16(2)	C14–C15–Ru	114.4(3)	C14–C15–W1	115.4(4)	C11–W1–C6	75.3(6)
C23–O4	1.154(6)	W1–C25	1.979(6)	O4–C20	1.15(2)	C23–Ru–C24	90.5(2)	C23–W1–C25	103.9(2)	C13–W1–C6	73.1(6)
C24–O3	1.148(7)	O3–C23	1.167(7)	O3–C13	1.15(2)	C23–Ru–C15	89.4(2)	C23–W1–C24	76.9(2)	C12–W1–C6	131.4(7)
C12–C11	1.519(6)	O4–C24	1.154(6)	O2–C12	1.15(2)	C24–Ru–C15	85.9(2)	C25–W1–C24	79.8(2)	C11–W1–C13	105.3(7)
C12–C13	1.525(6)	O5–C25	1.140(7)	O1–C11	1.16(2)			C23–W1–C15	74.2(2)	C11–W1–C12	75.6(7)
C14–C13	1.517(6)	C11–C12	1.515(8)	C6–C7	1.529(16)			C24–W1–C15	134.1(2)	C13–W1–C12	78.1(8)
C14–C15	1.520(6)	C13–C12	1.533(8)	C7–C8	1.530(15)			C25–W1–C15	73.6(2)	C7–C6–W1	118.1(10)
		C13–C14	1.538(8)	C9–C8	1.537(16)						
		C14–C15	1.536(8)	C9–C10	1.532(16)						

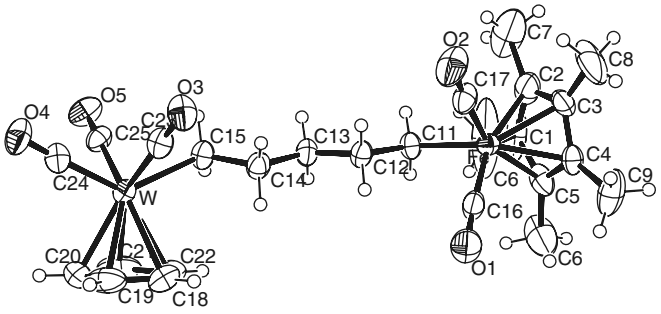

Fig. 6. The molecular structure of $[Cp^*(CO)_2Fe(CH_2)_5W(CO)_3Cp]$ (**3**) showing the atom numbering scheme. Note that the methyl groups on the Cp^* ligand are disordered.

suggest that similar geometry distortion as that observed in $[Cp^*(CO)_2Fe\{\mu\text{-}(C_3H_5)\}Ru(CO)_2Cp]PF_6$ (**1a**), may have occurred upon hydride abstraction. Efforts are being made to obtain X-ray quality crystals of the carbocation complexes. Crystal data and experimental details of data collection and refinement are given in Table 10.

The torsion angles C12–C13–C14–C15 = 170.1(5)°, Fe1–C11–C12–C13 = 178.1(4)°, C14–C13–C12–C11 = 175.8(5)°, and C13–C14–C15–W1 = 167.6(4)° confirm that the alkyl chain is fully saturated and σ-bonded to both transition metals.

The molecular structure of $[Cp(CO)_2Ru(CH_2)_5W(CO)_3Cp]$ (**4**) shown in Fig. 7 can be compared with both compounds **2** and **3**. It contains a ruthenium centre coordinated in the same way as in compound **2** and is linked to a tungsten centre by a pentanediyl chain in the same manner as in compound **3**. It differs from both complexes by having a "kink" in the alkyl chain (see Fig. 7). This strained *gauche* conformation has been observed in other organometallic complexes involving long chain alkyl groups such as the polymethylene-bridged cobaloximes [37,38]. It has also been reported in the alkyl substituent of the imidazolium salt 1,1′-[1,10-decyl]bis[3-methyl-1*H*-imidazolium-1-yl]hexafluorophosphate [39].

The bond length $Ru–C_{\alpha(alkyl)} = 2.138(16)$ Å falls within the range 2.13(2)–2.17(2) Å observed in compounds **1** and **2**. The $Ru–C_{CO}$ bonds are 1.85(2) Å and 1.847(19) Å and are within the range 1.84(4)–1.91(3) Å observed in compounds **1** and **2**. The bond length $W–C\alpha_{(alkyl)} = 2.320(16)$ Å is the same as that observed in compound **3**. Similarly, the $W–C_{CO}$ distances of 1.968(16) Å, 1.992(18) Å and 1.969(17) Å, respectively, fall within the range 1.960(6)–1.981(6) Å observed in compound **3**. The C–C bond distances within the alkyl chain are similar to those within the alkyl chain in compound **3**, but slightly longer than those in compound **2**. The Cp ligands are oriented almost perpendicular to one another, with the angle between the ring planes being 81°. Selected bond angles and bond distances are given in Table 9.

The torsion angles associated with the alkyl bridge are W–C6–C7–C8 = −168.9(11)°, C6–C7–C8–C9 = 70(2)°, C10–C9–C8–C7 = 175.4(16)°, and C8–C9–C10–Ru1 = −178.2(13)°. The significantly reduced angle C6–C7–C8–C9 = 70(2)° reflects the unusual kink in the alkyl chain.

3. Conclusions

We have shown, by ^1H and ^{13}C NMR spectroscopy, that in the mixed-ligand complexes $[Cp^*(CO)_2Fe(CH_2)_nM(CO)_xCp]$ ($n > 3$, $x = 2$, M = Fe, Ru; $x = 3$, M = W), hydride abstraction takes place selectively from the CH_2 group β to Fe attached to the Cp^* ligand. In the Ru–W complexes $[Cp(CO)_2Ru(CH_2)_nW(CO)_3Cp]$ where $n = 4$, 5 hydride abstraction was totally metalloselective, always taking place at the CH_2 group β to the Ru metal centre.

Table 10
Crystal data and experimental details for complexes **1**, **2**, **3** and **4**

Compound	**1**	**2**	**3**	**4**
Empirical formula	$C_{22}H_{26}FeO_4Ru$	$C_{24}H_{30}FeO_4Ru$	$C_{25}H_{30}FeO_5W$	$C_{25}H_{30}O_5RuW$
Formula weight (g/mol)	511.36	539.40	650.21	695.43
Lattice	Monoclinic	Monoclinic	Monoclinic	Monoclinic
Space group	$P2_1/c$	$C2/c$	$P2_1/c$	$P2_1/c$
a (Å)	26.57(2)	30.739(5)	12.5991(4)	22.241(9)
b (Å)	8.482(4)	8.2029(12)	12.4843(3)	7.747(2)
c (Å)	20.862(11)	23.649(4)	15.6910(5)	11.506(4)
α (°)	90.00	90.00	90.00	90.00
β (°)	112.35(6)	127.992(10)	105.798(3)	99.89(3)
γ (°)	90.00	90.00	90.00	90.00
V (Å^3)	4348(5)	4699.5(12)	2455.75(13)	1953.0(12)
Z	4	8	4	4
D_{calc} (Mg m^{-3})	1.562	1.525	1.759	2.127
Temperature (K)	150(2)	120(2)	150(2)	120(2)
Crystal size (mm)	$0.3 \times 0.3 \times 0.3$	$0.2 \times 0.2 \times 0.05$	$0.2 \times 0.15 \times 0.05$	$0.4 \times 0.4 \times 0.4$
F(000)	2080	2208	1280	1192
μ (Mo Kα) (mm^{-1})	1.385	1.286	5.303	6.686
Wavelength (λ)	0.71073 Å	0.71073 Å	0.71073 Å	0.71073 Å
Reflections for cell parameters	620	1003	852	1037
Crystal description	plate	plate	plate	plate
Crystal colour	Yellow	Yellow	Yellow	Pale yellow
Collected data of 2θ range (°)	4.15–29.67	4.20–31.87	3.60–34.34	4.42–29.92
Transmission factors (T_{min}, T_{max})	0.6814, 0.6814	0.7830, 0.9385	0.4168, 0.7774	0.1751; 0.1751
Measured reflections	31 194	23 427	39 720	18 899
Independent reflections	11 304	7528	9268	4981
Observed reflections with $I > 2\sigma(I)$	10 192	5324	4583	4752
Internal fit	$R_{int} = 0.0835$	$R_{int} = 0.0615$	$R_{int} = 0.0553$	$R_{int} = 0.0665$
h	$-36 \rightarrow 23$	$-45 \rightarrow 35$	$-18 \rightarrow 18$	$-28 \rightarrow 30$
k	$-11 \rightarrow 11$	$-11 \rightarrow 12$	$-17 \rightarrow 19$	$-9 \rightarrow 10$
l	$-27 \rightarrow 28$	$-29 \rightarrow 33$	$-24 \rightarrow 24$	$-13 \rightarrow 15$
Final R indices [$F^2 > 2\sigma(F^2)$]	$R_1 = 0.2515$, $wR(F^2) = 0.5441$	$R_1 = 0.0619$, $wR(F^2) = 0.1448$	$R_1 = 0.0501$, $wR(F^2) = 0.1254$	$R_1 = 0.0956$, $wR(F^2) = 0.2203$
Goodness-of-fit on F^2(S)	1.124	1.208	0.899	1.147
Parameters	280	276	294	244
Maximum shift	$(\Delta/\sigma)_{max} = 0.011$	$(\Delta/\sigma)_{max} = 0.001$	$(\Delta/\sigma)_{max} = 0.063$	$(\Delta/\sigma)_{max} = 0.001$
Largest difference in peak (e Å^{-3})	$\Delta\rho_{max} = 6.602$	$\Delta\rho_{max} = 1.203$	$\Delta\rho_{max} = 5.453$	$\Delta\rho_{max} = 6.674$
Largest hole (e Å^{-3})	$\Delta\rho_{min} = -5.814$	$\Delta\rho_{min} = -0.503$	$\Delta\rho_{min} = -0.918$	$\Delta\rho_{min} = -6.480$

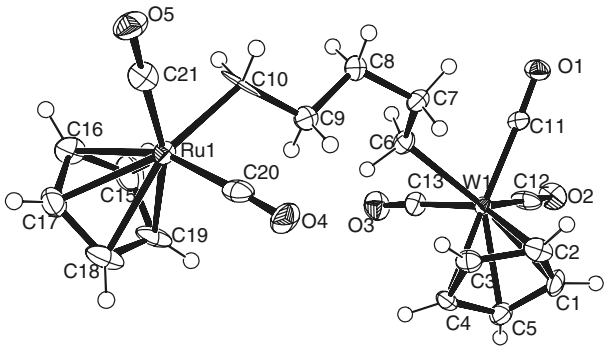

Fig. 7. The molecular structure of $[Cp(CO)_2Ru(CH_2)_5W(CO)_3Cp]$ (**4**) showing the atom numbering scheme. Note that the methyl C10 and C21 are disordered.

Single crystal X-ray crystallography data have also revealed that hydride abstraction leads to distortion of the molecular geometry to allow increased interaction between one metal centre and the formally positive β-CH^+ carbon, resulting in the formation of a metallacyclopropane type of structure. The carbocation complexes are chiral with the β-CH carbon being the chiral centre according to ^{1}H and ^{13}C NMR data. This is further strong evidence supporting the proposed metallacyclopropane bonding model. ^{13}C NMR data have also shown that the positive charge in the cationic metallacyclic complexes is delocalized mainly within the metallacyclopropane ring.

The cationic metallacyclic complexes $[Cp^*(CO)_2Fe\{\mu\text{-}(C_nH_{2n-1})\}ML_y]PF_6$ where $n > 3$ behave like ionic liquids. They collect as red oils upon addition of diethyl ether to their CH_2Cl_2 solutions and attempts to dry them under reduced pressure leads to the formation of low melting spongy solids. This is not unexpected given the fact that the cations, $[Cp^*(CO)_2Fe\{\mu\text{-}(C_nH_{2n-1})\}ML_y]^+$, are large, while the associated counter anion PF_6^- is relatively small.

4. Experimental

4.1. General

All reactions were carried out under inert atmosphere (UHP or HP nitrogen) using standard Schlenk tube techniques. Heptane (Rochelle >98%) was distilled from sodium/benzophenone ketyl and stored over sodium wire. Decane and diglyme were dried over sodium wire and used without distillation. The molecular sieves 4 Å (Merck AR) were dried in a tube furnace at 250 °C for 10 h and cooled in a dessiccator before use. The other solvents were treated as previously reported [27].

Dicyclopentadiene (Fluka 95%), iron pentacarbonyl (Aldrich), pentamethylcyclopentadiene (Aldrich 95%), $RuCl_3 \cdot xH_2O$ (Johnson Matthey), tungsten hexacarbonyl (Acros 99%), pentane, ferric sulfate (Merck AR), glacial acetic acid (Kleber 99.5%), mercury (Associated Chemical Enterprises, triple distilled AR), 1,3-dibromopropane (Aldrich 99%), 1,4-dibromobutane (Fluka 98%), 1,5-dibromopentane (Aldrich 97%), and 1,6-dibromohexane (Aldrich 98%) were used as purchased. Sodium iodide was dried under reduced pressure at 100 °C for 8 h before use. Alumina (Merck, aluminium oxide 90 neutral, active) was deactivated with deionized water and dried in an oven kept at 110 °C before use. Melting points were recorded on an Ernst Leitz Wetzlar hot-stage microscope and are uncorrected. Elemental analyses were performed on a LECO CHNS-932 elemental analyzer. Infrared spectra were recorded on a Nicolet Impact 400D 5DXFT-spectrophotometer between 4000–400 cm^{-1}, either in solution using liquid cell, NaCl windows (Aldrich 99.99%) or KBr (Aldrich 99.99%) discs. NMR spectra were recorded on Varian Gemini 300 MHz and Varian Inova 400 MHz spectrometer. Variable temperature NMR spectra were recorded on a Varian Inova 500 MHz spectrometer. The solvents, $CDCl_3$ (Aldrich, 99.8%), acetone-d_6 (Aldrich, 99.5%), acetonitrile-d_3 (Aldrich, 99.8%), and *N*,*N*-dimethylformamide-d_7 (Aldrich, 99.5%) were used as purchased or occasionally dried over type 4A molecular sieves. Solutions for NMR spectroscopy were always prepared under nitrogen gas using nitrogen-saturated solvents.

The precursors $Ru_3(CO)_{12}$ [40], $[Cp(CO)_2Fe]_2$ [41], $[Cp(CO)_2Ru]_2$ [42], and $[Cp(CO)_3W]_2$ [43] were prepared by the literature methods. $[Cp^*(CO)_2Fe]_2$ was either purchased from Strem chemicals or prepared by the modified literature method [44]. The halogenoalkyl complexes $[Cp(CO)_2Fe\{(CH_2)_nX\}]$ (X = Br, I; $n = 3$–6) [45], $[Cp(CO)_2Ru\{(CH_2)_nX\}]$ (X = Br, I, $n = 3$–6) [46], and $[Cp(CO)_3W\{(CH_2)_nX\}]$ (X = Br, I; $n = 3$–6) [47] were prepared by the literature methods and used to prepare the mixed-ligand alkanediyl complexes.

4.2. Preparation of $[Cp^*(CO)_2Fe]_2$

Pentamethylcyclopentadiene (1 mL) was added to a solution of iron pentacarbonyl (2 mL) in nitrogen-saturated *n*-decane (30 mL) in a Schlenk tube. The mixture was refluxed for 24 h at 160 °C and then allowed to cool to room temperature over several hours. A shiny black solid precipitated and was filtered off in air, washed with hexane (10 mL) and dried under reduced pressure. It was extracted several times with dichloromethane until the extracts were clear (about 150 mL) and a dark maroon solution was obtained. The solvent was removed under reduced pressure to give a maroon solid, which was found to be analytically pure, and its IR spectrum in CH_2Cl_2 and elemental analysis data matched those of an authentic sample (Strem Chemicals).

4.3. Preparation of $[Cp^*(CO)_2Fe(CH_2)_nFe(CO)_2Cp]$ ($n = 3$–6)

These were prepared by the modified literature method [28]. For example, a solution of $Na[Cp^*(CO)_2Fe]$ (1.5 mmol) in THF was added to a stirred solution of $[Cp(CO)_2Fe\{(CH_2)_3I\}]$ (0.76 g, 2.1 mmol) in THF at −78 °C. The mixture was stirred at this temperature for 20 min and then allowed to attain room temperature, while monitoring the reaction by IR spectroscopy (ν(CO)). When the reaction was judged complete (after 5 h), the solvent was removed under reduced pressure leaving a brown solid. This solid was extracted three times with 20 mL portions of hexane and the solution concentrated under reduced pressure to about 10 mL. A yellow solid formed. The mother liquor was syringed off, the solid washed once with 3 mL ice-cold hexane and dried under reduced pressure. Analytical and spectroscopic data matched that of the reported compound [28]. The complexes where $n = 4$–6 were prepared in a similar manner. These are new and their characterization data are reported here.

$[Cp^*(CO)_2Fe(CH_2)_4Fe(CO)_2Cp]$: Yield = 54% based on the haloalkyl complex, IR ν(CO) (hexane): (cm^{-1}) 2008s, 1987s, 1953s, 1932s. Anal. Calc. for $C_{23}H_{28}Fe_2O_4$: C, 57.53; H, 5.87. Found: C, 56.97; H, 5.77%. ^{1}H NMR ($CDCl_3$): [δ] 4.70s (5H, *Cp*Fe), 1.70s (15H, *Cp**Fe), 1.33–1.43m (6H, $CpFeCH_2CH_2CH_2$), 0.91t (2H, Cp^*FeCH_2), ^{13}C NMR ($CDCl_3$): [δ] 219.7 (Cp^*FeCO), 217.9 (CpFe*C*O), 94.7 ($C_5(CH_3)_5$), 85.3 (*Cp*Fe), 45.1 ($Cp^*FeCH_2CH_2$), 43.6 ($Cp^*FeCH_2CH_2CH_2$), 14.1 (Cp^*FeCH_2), 4.1 ($CpFeCH_2$).

$[Cp^*(CO)_2Fe(CH_2)_5Fe(CO)_2Cp]$: Yield = 64% based on the haloalkyl complex, IR ν(CO) (hexane): (cm^{-1}) 2008s, 1985s, 1955s, 1938s; ^{1}H NMR ($CDCl_3$): [δ] 4.69s (5H, *Cp*Fe), 1.70s (15H, *Cp**Fe), 1.34–1.43m (8H, $CpFeCH_2CH_2CH_2CH_2$), 0.91t (2H, Cp^*FeCH_2); ^{13}C NMR ($CDCl_3$): [δ] 219.7(Cp^*FeCO), 217.8 (CpFe*C*O), 94.7 ($C_5(CH_3)_5$), 85.3 (*Cp*Fe), 41.3 ($Cp^*FeCH_2CH_2CH_2$), 38.4 ($Cp^*FeCH_2CH_2$), 37.7 ($CpFeCH_2CH_2$), 14.2 ($FeCH_2$), 9.3 ($C_5(CH_3)_5$), 4.1 ($CpFeCH_2$).

$[Cp^*(CO)_2Fe(CH_2)_6Fe(CO)_2Cp]$ was only identified by its IR (hexane) data (2008, 1986, 1953, 1932) and used for the preparation of the cationic metallacyclic complex without further characterization.

4.4. Preparation of $[Cp^*(CO)_2Fe\{\mu\text{-}(C_nH_{2n-1})\}Fe(CO)_2Cp]PF_6$ ($n = 3$–6)

A filtered solution of Ph_3CPF_6 (0.38 g, 0.95 mmol) in CH_2Cl_2 (10 mL) was added to a solution of $[Cp^*(CO)_2Fe\text{-}(CH_2)_3Fe(CO)_2Cp]$ (0.44 g, 0.95 mmol) in CH_2Cl_2 (2 mL) in a Schlenk tube and the mixture allowed to stand overnight under nitrogen at room temperature. The resultant deep orange solution was filtered through a cannula into a pre-weighed Schlenk tube. Dry nitrogen-saturated diethyl ether was added to the solution until precipitation just started. The mixture was allowed to stand for about 1 h in the dark during which time a microcrystalline orange solid precipitated. The mother liquor was syringed off and the solid dried under reduced pressure. The rest of the complexes were prepared in the same manner, but instead of adding diethyl slowly and leaving the mixture for 1 h, the diethyl ether was added rapidly, during which time the compounds separated out as red oils. The mother liquor was syringed off and the compounds dried under reduced pressure. As soon as the vacuum was applied the red oils swelled up to spongy pale yellow solids, which were found to be analytically pure. Yields and other characterization data are given in Table 1.

4.5. Preparation of $[Cp^*(CO)_2Fe(CH_2)_nRu(CO)_2Cp]$ ($n = 3$–6)

These compounds were prepared following the same procedure described in Section 4.3, using the salt $Na[Fe(CO)_2Cp^*]$ and the iodoalkyl ruthenium complexes $[Cp(CO)_2Ru(CH_2)_nI]$. The characterization data of the complexes where $n = 3$–5 matched the literature data [28]. The molecular structure of $[Cp^*(CO)_2Fe\{\mu\text{-}(CH_2)_5\}Ru(CO)_2Cp]$ has been confirmed by single crystal X-ray crystallography. The complex $[Cp^*(CO)_2Fe(CH_2)_6Ru(CO)_2Cp]$ is new and thus its characterization data are reported here.

Yield = 57% based on the iodoalkyl complex, IR (hexane): (cm^{-1}) 2018s, 1988s, 1959s, 1933s; ^1H NMR ($CDCl_3$): [δ] 5.20s (5H, *Cp*Ru), 1.70s (15H, *Cp**Fe), 1.54m (2H, RuC*H*$_2$), 1.43m (2H, RuCH$_2$CH$_2$C*H*$_2$), 1.31m (2H, FeCH$_2$C*H*$_2$), 1.34m (2H, FeCH$_2$CH$_2$C*H*$_2$), 1.31m (2H, RuCH$_2$C*H*$_2$), 0.91t (2H, FeC*H*$_2$); ^{13}C NMR ($CDCl_3$): [δ] 219.7(Cp*Fe*C*O), 202.6 (Ru*C*O), 94.7 (*C*$_5$(CH$_3$)$_5$), 88.6 (*Cp*M), 40.0 (RuCH$_2$CH$_2$-*C*H$_2$), 37.9 (FeCH$_2$CH$_2$*C*H$_2$), 35.5 (FeCH$_2$*C*H$_2$), 34.4 (RuCH$_2$*C*H$_2$), 9.3 (C$_5$(*C*H$_3$)$_5$), 14.2 (Fe*C*H$_2$), −2.9 (Ru*C*H$_2$).

4.6. Preparation of $[Cp^*(CO)_2Fe\{\mu\text{-}(C_nH_{2n-1})\}Ru(CO)_2Cp]PF_6$ ($n = 3$–6)

All the reactions were carried out by following the procedure described in Section 4.4.

4.7. Preparation of $[Cp^*(CO)_2Fe(CH_2)_nW(CO)_3Cp]$ ($n = 3$–6)

These new compounds were prepared in a similar manner as the iron-ruthenium complexes $[Cp^*(CO)_2Fe(CH_2)_n\text{-}Ru(CO)_2Cp]$ (Section 4.5), using the salt $Na[Cp^*(CO)_2Fe]$ and the tungsten iodoalkyl complexes $[Cp(CO)_3W\text{-}\{(CH_2)_nI\}]$. The molecular structure of $[Cp^*(CO)_2Fe\text{-}\{\mu\text{-}(CH_2)_5\}W(CO)_3Cp]$ has been confirmed by single crystal X-ray crystallography. The complexes have been characterized by IR and NMR spectroscopy and elemental analysis as follows:

$[Cp^*(CO)_2Fe(CH_2)_3W(CO)_3Cp]$: Yield = 72%, Decomposes >120 °C, IR (CH_2Cl_2): (cm^{-1}) 2005, 1976, 1918; ^1H NMR ($CDCl_3$): [δ] 5.61s (5H, CpW), 1.77s (15H, C$_5$*Me*$_5$Fe), 1.69m (4H, WC*H*$_2$C*H*$_2$), 0.99t (2H, FeC*H*$_2$); ^{13}C NMR ($CDCl_3$): [δ] 218.4 (Cp*Fe–CO), 219.6, 229.7 (CpW–CO), 91.9 (CpW), 94.8 (*C*$_5$Me$_5$Fe), 18.9 (Fe*C*H$_2$), 44.9 (FeCH$_2$*C*H$_2$), −4.7 (W*C*H$_2$), 8.2 (C$_5$(*C*H$_3$)$_5$Fe).

$[Cp^*(CO)_2Fe(CH_2)_4W(CO)_3Cp]$: Yield = 56%; M.p. = 126–128 °C; IR (hexane): (cm^{-1}) 2014, 1987, 1929, 1761. Anal. Calc. for $C_{24}H_{28}FeO_5W$: C, 45.31; H, 4.44. Found: C, 45.35; H, 4.46%. ^1H NMR ($CDCl_3$): [δ] 5.35s, (5H, CpW), 1.70s (15H, C$_5$*Me*$_5$Fe), 1.55m (4H, WC*H*$_2$ and FeCH$_2$C*H*$_2$), 1.43m (2H, WCH$_2$C*H*$_2$), 0.99t (2H, FeC*H*$_2$); ^{13}C NMR ($CDCl_3$): [δ] 219.6, 229.7 (CpW–CO), 218.4 (Cp*Fe–CO), 94.8 (*C*$_5$Me$_5$Fe), 91.9 (CpW), 44.9 (FeCH$_2$*C*H$_2$), 18.9 (Fe*C*H$_2$), 8.2 (C$_5$ (*C*H$_3$)$_5$Fe), −4.7 (W*C*H$_2$).

$[Cp^*(CO)_2Fe(CH_2)_5W(CO)_3Cp]$: Yield = 82%, M.p. = 125–127 °C; IR (hexane): (cm^{-1}) 2008, 1978, 1916. Anal. Calc. for $C_{25}H_{30}FeO_5W$: C, 46.18; H, 4.65. Found: C, 46.22 H 4.59%. ^1H NMR ($CDCl_3$): [δ] 5.34s, (5H, CpW), 1.70s (15H, C$_5$*Me*$_5$Fe), 1.53m (2H, WC*H*$_2$) 1.31m (2H, WCH$_2$C*H*$_2$), 0.99t (2H, FeC*H*$_2$), 1.43m (FeCH$_2$C*H*$_2$C*H*$_2$), ^{13}C NMR ($CDCl_3$): [δ] 219.7, 229.4 (CpW–CO), 217.4 (Cp*Fe–CO), 94.8 (*C*$_5$Me$_5$Fe), 91.5 (CpW), 42.2 (FeCH$_2$CH$_2$*C*H$_2$), 37.3 (FeCH$_2$*C*H$_2$), 36.9 (WCH$_2$*C*H$_2$), 14.2 (Fe*C*H$_2$), 9.3 (C$_5$ (*C*H$_3$)$_5$Fe), −4.7 (W*C*H$_2$).

$[Cp^*(CO)_2Fe\{\mu\text{-}(CH_2)_6\}W(CO)_3Cp]$ was only identified by its IR ν(CO) (hexane) data (2009, 1975, 1915 cm^{-1}) and converted to the cationic metallacyclic complex.

4.8. Preparation of $[Cp^*(CO)_2Fe\{\mu\text{-}(C_nH_{2n-1})\}W(CO)_3Cp]PF_6$ ($n = 3$–5)

These reactions were carried out in a similar manner to those of the mixed-ligand heterobimetallic complexes of iron and ruthenium described in Section 4.4.

4.9. Preparation of $[Cp(CO)_2Ru\{\mu\text{-}(CH_2)_n\}W(CO)_3Cp]$ ($n = 3$–6)

The preparation of the complex $[Cp(CO)_2Ru(CH_2)_3W\text{-}(CO)_3Cp]$ will be described to illustrate the general method used in the preparation of these new compounds. A solution of $Na[Cp(CO)_2Ru]$ (0.80 mmol) in THF (15 mL) was added to a solution of the iodoalkyl complex $[Cp(CO)_3W\{(CH_2)_3I\}]$ (0.4 g, 0.80 mmol) in THF (3 mL)

at −30 °C over a period of 10 min. The solution was stirred at this temperature for 20 min and then allowed to attain room temperature (1 h) and stirred for a further 8 h. The solution was the concentrated at reduced pressure to leave a brown solid. This was extracted three times with a 1:1 mixture of hexane and CH_2Cl_2 (3 × 20 mL) and a pale yellow solution was obtained. The solvent was concentrated under reduced pressure to about a third of the original volume and then cooled to −78 °C, when a pale yellow solid precipitated. The mother liquor was syringed off and the solid dried under reduced pressure. The complexes where $n = 4$, 5 were prepared similarly. The molecular structure of $[Cp(CO)_2Ru(CH_2)_5W(CO)_3Cp]$ has been confirmed by single crystal X-ray crystallography. The complexes where $n = 3$–5 have been characterized by IR, NMR spectroscopy and elemental analysis as follows:

$[Cp(CO)_2Ru(CH_2)_3W(CO)_3Cp]$: Yield = 50% based on the haloalkyl precursor; IR(CH_2Cl_2): (cm^{-1}) 2007m, 1943m, 1910s; M.p. = 125–127 °C. Anal. Calc. for $C_{18}H_{16}O_5RuW$: C, 36.20; H, 2.70. Found: C, 36.25; H, 2.73%. ^1H NMR ($CDCl_3$): [δ] 5.35s (5H, *Cp*W), 5.21s (5H, *Cp*Ru), 1.72m (2H, $RuCH_2CH_2$), 1.68m (2H, $RuCH_2$), 1.56t (WCH_2); ^{13}C NMR($CDCl_3$): [δ] 229.3, 217.6 (W*C*O), 202.6 (Ru*C*O), 91.3 (*Cp*W), 88.5 (*Cp*Ru), 47.2 ($RuCH_2CH_2$), 2.4 ($RuCH_2$), −5.5 (WCH_2).

$[Cp(CO)_2Ru(CH_2)_4W(CO)_4Cp]$: Yield = 39% based on the haloalkyl precursor; IR(CH_2Cl_2): (cm^{-1}) 2009m, 1944m, 1911s; M.p. = 120–122 °C. Anal. Calc. for $C_{19}H_{18}O_5RuW$: C, 37.33; H, 2.97. Found: C, 37.34; H, 2.93%. ^1H NMR ($CDCl_3$): [δ] 5.35s (5H, *Cp*W), 5.20s (5H, *Cp*Ru), 1.66m (2H, $RuCH_2$), 1.53m (6H, $WCH_2CH_2CH_2$); ^{13}C NMR ($CDCl_3$): [δ] 229.3, 217.5 (W*C*O), 202.6 (Ru*C*O), 91.5 (*Cp*W), 88.6 (*Cp*Ru), 46.2 ($RuCH_2CH_2$), 42.4 ($RuCH_2CH_2CH_2$), −3.7 ($RuCH_2$), −9.8 (WCH_2).

$[Cp(CO)_2Ru(CH_2)_5W(CO)_3Cp]$: Yield = 56% based on the haloalkyl; IRν(CO)/CH_2Cl_2: (cm^{-1}) 2009m, 1944m, 1911s; M.p. = 68–70 °C. Anal. Calc. for $C_{20}H_{20}O_5RuW$: C, 38.42; H, 3.22. Found: C, 37.98, H 3.48%. ^1H NMR ($CDCl_3$): [δ] 5.35s (5H, *Cp*W), 5.21s (5H, *Cp*Ru), 1.66m (2H, $RuCH_2$), 1.52m (2H, $RuCH_2CH_2$); 1.53m ($RuCH_2CH_2CH_2$), 1.53m (WCH_2), 1.25m (WCH_2CH_2) ^{13}C NMR ($CDCl_3$): [δ] 229.3, 217.5 (W*C*O), 202.6 (Ru*C*O), 91.5 (*Cp*W), 88.6 (*Cp*Ru), 41.2 ($RuCH_2CH_2$), 39.5 ($RuCH_2CH_2CH_2$), 36.8 (WCH_2CH_2) −9.8 (WCH_2), −3.2 ($RuCH_2$).

$[Cp(CO)_2Ru(CH_2)_6W(CO)_3Cp]$ was only identified by its IR(CH_2Cl_2) (cm^{-1}) data (2009, 1975, 1915 cm^{-1}) and converted to the cationic metallacyclic complex without further characterization.

4.10. Preparation of $[Cp(CO)_2Ru\{\mu\text{-}(C_nH_{2n-1})\}W(CO)_3Cp]PF_6$ (n = 3–6)

These were carried out in a similar manner as explained in Section 4.4. Pale yellow microcrystalline solids were obtained.

4.11. Reactions of some of the complexes $[Cp^*(CO)_2Fe\{\mu\text{-}(C_5H_9)\}M(CO)_2Cp]PF_6$ (M = Fe or Ru) with sodium iodide

Approximately 10 mg of a given complex was dissolved in N_2-saturated deuterated acetone in an NMR tube and its ^1H NMR spectrum recorded. About 10 mg of NaI was added to the solution in the NMR tube and the reaction followed by recording spectra at 5-min intervals until there was no further change observed in the spectra. $[Cp^*(CO)_2Fe\{\mu\text{-}(C_5H_9)\}Fe(CO)_2Cp]PF_6$ gave $Cp^*(CO)_2FeI$ and the previously reported $[Cp(CO)_2FeCH_2(CH_2)_2CH{=}CH_2]$ [36], as recognized by their ^1H NMR spectra as follows:

$Cp^*(CO)_2FeI$: [δ] 2.01s ($C_5(CH_3)_5$).

$[Cp(CO)_2FeCH_2(CH_2)_2CH{=}CH_2]$: [$\delta$] 4.92s (Cp), 1.45m ($Fe(CH_2)_3CH_2$), 2.06m ($Fe(CH_2)_3CH_2$), 5.04m ($FeCH_2(CH_2)_2CH{=}CH_2$), 5.82m ($FeCH_2(CH_2)_2CH{=}CH_2$). Unreacted $[Cp^*(CO)_2Fe\{\mu\text{-}(C_5H_9)_n\}Fe(CO)_2Cp]PF_6$ was also observed in solution.

$[Cp^*(CO)_2Fe\{\mu\text{-}(C_5H_9)_n\}Ru(CO)_2Cp]PF_6$ gave $Cp^*(CO)_2FeI$ and the new σ-alkenyl complex $[Cp(CO)_2RuCH_2(CH_2)_2CH{=}CH_2]$, as recognized by its ^1H NMR spectrum as follows: [δ] 5.42s (CpRu), 1.58m ($Ru(CH_2)_3CH_2$), 2.20m ($Ru(CH_2)_3CH_2$), 4.91m ($RuCH_2(CH_2)_2CH{=}CH_2$), 5.80m ($RuCH_2(CH_2)_2CH{=}CH_2$). Unreacted $[Cp^*(CO)_2Fe\{\mu\text{-}(C_5H_9)\}Ru(CO)_2Cp]PF_6$ was also observed in solution.

4.12. Reaction of $[Cp^*(CO)_2Fe\{\mu\text{-}(C_5H_9)\}\text{-}Ru(CO)_2Cp]PF_6$ with CD_3OD

Approximately 10 mg of the complex was dissolved in N_2-saturated deuterated methanol in an NMR tube and its ^1H NMR spectrum recorded. About 10 mg of Na_2CO_3 was added to the solution in the NMR tube and the reaction followed by recording spectra at 5-min intervals until there was no further change observed in the spectra. Most of the complex had reacted after 40 min, but the reaction did not go to completion. Four compounds were observed in solution: $[Cp^*(CO)_2Fe]_2$, $[Cp^*(CO)_2FeOCD_3]$, unreacted $[Cp^*(CO)_2Fe\{\mu\text{-}(C_5H_9)\}Ru(CO)_2Cp]PF_6$ and the new complex $[Cp(CO)_2RuCH_2(CH_2)_2CH{=}CH_2]$, as identified by their ^1H NMR spectra as follows: *$[Cp^*(CO)_2Fe]_2$*: 1.77s ($C_5(CH_3)_5$); *$[Cp^*(CO)_2FeOCD_3]$*, 1.80s ($C_5(CH_3)_5$), *$[Cp(CO)_2RuCH_2(CH_2)_2CH{=}CH_2]$*: [$\delta$] 5.36s (CpRu), 1.68m {$Ru(CH_2)_3CH_2$}, 2.08m {$Ru(CH_2)_3CH_2$}, 5.01m {$RuCH_2(CH_2)_2CH{=}CH_2$}, 5.82m ($RuCH_2(CH_2)_2CH{=}CH_2$).

4.13. Reactions of the complexes $[Cp^*(CO)_2Fe\{\mu\text{-}(C_5H_9)\}W(CO)_3Cp]PF_6$ and $[Cp^*(CO)_2Fe\{\mu\text{-}(C_5H_9)\}Fe(CO)_2Cp]PF_6$ with $NaBPh_4$

The complex $[Cp^*(CO)_2Fe\{\mu\text{-}(C_5H_9)\}W(CO)_3Cp]PF_6$ (0.038 g, 0.048 mmol) and $NaBPh_4$ (0.016 g, 0.085 mmol) were weighed into a Schlenk tube followed by 10 mL acetone. The mixture was stirred for 10 min. The solvent was removed under reduced pressure to leave a yellow

solid. This was extracted twice with 10 mL portions of CH_2Cl_2 and filtered through a cannula into a pre-weighed Schlenk tube. Diethyl ether was added to the solution to precipitate the product as thin yellow plates. The mother liquor was syringed off and the solid dried under reduced pressure. The complex $[Cp^*(CO)_2Fe\{\mu\text{-}(C_5H_9)\}Fe(CO)_2Cp]PF_6$ was treated similarly and gave $[Cp^*(CO)_2Fe\{\mu\text{-}(C_5H_9)\}Fe(CO)_2Cp]BPh_4$.

4.14. X-ray crystal structure determinations of complexes 1–4

Single crystals of **1**–**4** suitable for X-ray diffraction studies were obtained by slow evaporation of solvent from concentrated hexane solutions of the compounds held at 278 K over a period of 5–7 weeks. The X-ray diffraction intensity data were collected with an Oxford Excalibur 2 diffractometer (CrysAlis CCD 170) using Mo **K**α radiation ($\lambda = 0.71073$ Å) with a ω–2θ scan mode [48]. The structures were solved by direct methods using SHELXS-97 [49] and refined using SHELXL-97 [49]. The details of the crystallographic data and the procedures used for data collection and reduction information for compounds **1**–**4** are given in Table 10.

Acknowledgements

We acknowledge financial support from NRF, THRIP, and UKZN (URF). One of us (E.O.C.) thanks Kenyatta University, Kenya, for study leave to carry out this work. We thank Drs. A.W.F. Kamdem (University of Douala, Cameroun), G.E.M. Maguire (UKZN) and H.G. Kruger (UKZN) for fruitful NMR discussions.

Appendix A. Supplementary material

CCDC 630865, 630866, 630867 and 630868 contain the supplementary crystallographic data for compounds **1**, **2**, **3** and **4**. These data can be obtained free of charge via http://www.ccdc.cam.ac.uk/conts/retrieving.html, or from the Cambridge Crystallographic Data Centre, 12 Union Road, Cambridge CB2 1EZ, UK; fax: (+44) 1223-336-033; or e-mail: deposit@ccdc.cam.ac.uk. Supplementary data associated with this article can be found, in the online version, at doi:10.1016/j.jorganchem.2007.02.016.

References

[1] E.O. Changamu, H.B. Friedrich, M. Rademeyer, Acta Crystallogr., Sect. E 62 (2006) m442.
[2] H.B. Friedrich, E.O. Changamu, M. Rademeyer, Acta Crystallogr., Sect. E 62 (2006) m405.
[3] M.L.H. Green, P.L.I. Nagy, J. Organomet. Chem. 1 (1963) 58.
[4] M.L.H. Green, P.L.I. Nagy, J. Am. Chem. Soc. 84 (1962) 1310.
[5] M.L.H. Green, P.L.I. Nagy, J. Chem. Soc. (1963) 189.
[6] H.S. Clayton, J.R. Moss, M.E. Dry, J. Organomet. Chem. 688 (2003) 181.
[7] D.E. Laycock, J. Hartgerink, M.C. Baird, J. Org. Chem. 45 (1980) 291.
[8] A. Curtler, D. Ehntholt, W.P. Giering, ; P. Lennon, S. Raghu, A. Rosan, M. Rosenblum, J. Tancrede, D. Wells, J. Am. Chem. Soc. 98 (1976) 3495.
[9] A. Curtler, D. Ehntholt, P. Lennon, K. Nicholas, D.F. Marten, M. Madhavarao, S. Raghu, A. Rosan, M. Rosenblum, J. Am. Chem. Soc. 97 (1975) 3149.
[10] J.W. Faller, B.V. Johnson, J. Organomet. Chem. 88 (1975) 101.
[11] H.B. Friedrich, R.A. Howie, M. Laing, M.O. Onani, J. Organomet. Chem. 689 (2004) 181.
[12] B.H. Friedrich, J.R. Moss, J. Chem. Soc., Dalton Trans. (1993) 2863.
[13] D. Dooling, G. Joorst, S.F. Mapolie, Polyhedron 20 (2001) 467.
[14] J.W. Johnson, J.R. Moss, Polyhedron 4 (1985) 563.
[15] P. Lennon, M. Rosenblum, J. Am. Chem. Soc. 105 (1983) 1233.
[16] S.-M. Peng, A.M. Arif, J.A. Gladysz, J. Chem. Soc., Dalton Trans. (1995) 1857, and references cited therein.
[17] J.P. Collman, L.S. Hegedus, J.R. Norton, R.G. Finke, Principles and Applications of Organotransition Metal Chemistry, University Science Books, Mill Valley, CA, 1987.
[18] R.D. Adams, Polyhedron 7 (1988) 2251.
[19] M.J.S. Dewar, Bull. Soc. Chim. Fr. 18 (1951) C79.
[20] J. Chatt, L.A. Duncanson, J. Chem. Soc. (1953) 2339.
[21] R. Hoffmann, M.M.L. Chen, D.L. Thorn, J. Am. Chem. Soc. 16 (1977) 503.
[22] B.E.R. Schilling, R. Hoffmann, J. Am. Chem. Soc. 101 (1979) 3456.
[23] Y. Jean, A. Lledos, J.K. Burdett, R. Hoffmann, J. Am. Chem. Soc. 110 (1988) 4506.
[24] U. Pidun, G. Frenking, Organometallics 14 (1995) 5325.
[25] G. Frenking, U. Pidun, J. Chem. Soc., Dalton Trans. (1997) 1653.
[26] W. Scherer, G. Eickerling, D. Shorokhov, E. Gullo, G.S. McGrady, P. Sirsch, New J. Chem. 30 (2006) 309, and references cited therein.
[27] E.O. Changamu, H.B. Friedrich, J. Organomet. Chem. 692 (2007) 1138.
[28] H.B. Friedrich, J.R. Moss, B.K. Williamson, J. Organomet. Chem. 394 (1990) 313.
[29] H.B. Friedrich, R.A. Howie, M.O. Onani, Acta Crystallogr., Sect. E 59 (2003) m145.
[30] H.B. Friedrich, M.O. Onani, M. Rademeyer, Acta Crystallogr., Sect. E 60 (2004) m551.
[31] R.O. Hill, C.F. Marais, J.R. Moss, K.J. Naidoo, J. Organomet. Chem. 587 (1999) 28.
[32] M. Laing, J.R. Moss, J. Johnson, J. Chem. Soc., Chem. Commun. (1977) 656.
[33] L. Pope, P. Sommerville, M. Laing, K.J. Hindson, J.R. Moss, J. Organomet. Chem. 112 (1976) 309.
[34] K.P. Finch, J.R. Moss, M.L. Niven, Inorg. Chim. Acta 166 (1989) 181.
[35] M. Cais, S. Dani, F.H. Herbstain, M. Kapon, J. Am. Chem. Soc. 100 (1978) 5554, and references cited therein.
[36] G. Joorst, R. Karlie, S.F. Mapolie, S. Afr. J. Chem. 51 (1998) 132.
[37] B.D.Y. Gupta, R.D. Mandal, Organometallics 25 (2006) 706.
[38] X. Zhang, Y. Li, Y. Mei, H. Chen, J. Organomet. Chem. 691 (2006) 659.
[39] J.D. Holbrey, A.E. Visser, S.K. Spear, W.M. Reichert, R.P. Swatloski, G.A. Broker, R.D. Rogers, Green Chem. 5 (2003) 129.
[40] M.I. Bruce, J.G. Matisons, R.C. Mallis, J.M. Partrick, B.W. Skelton, A.H. White, J. Chem. Soc., Dalton Trans. (1983) 2365.
[41] R.B. King, F.G.A. Stone, Inorg. Synth. 7 (1963) 110.
[42] N.M. Doherty, S.A.R. Knox, Inorg. Synth. 25 (1989) 179.
[43] A.R. Manning, P. Hackett, R. Birdwhistel, P. Soye, Inorg. Synth. 28 (1990) 148.
[44] R.B. King, M.B. Bisnette, J. Organomet. Chem. 8 (1967) 287.
[45] H.B. Friedrich, P.A. Makhesha, J.R. Moss, B.K. Williamson, J. Organomet. Chem. 384 (1990) 325.

[46] H.B. Friedrich, K.P. Finch, M.A. Gafoor, J.R. Moss, Inorg. Chim. Acta 206 (1993) 225.
[47] H.B. Friedrich, M.O. Onani, O.Q. Munro, J. Organomet. Chem. 633 (2001) 39.
[48] Oxford Diffraction, Oxford Diffraction Ltd., Xcalibur CCD System, CrysAlis Software system, Version 1.170, 2003.
[49] G.M. Sheldrick, SHELXS-97 and SHELXL-97, University of Göttingen, Göttingen, Germany, 1997.